

Modeling Connections of Small Frames - Static and Dynamic Analyses

C. Azoury¹

¹ Mechanical Engineering Department,
Lebanese University, Lebanon

A. Kallassy²,

² Civil Engineering Department,
Lebanese University, Lebanon

I. Moukarzel³

³ Faculty of Engineering,
Lebanese University, Lebanon

Abstract — The paper presents a proposal to create a new 1D linear finite element to substitute the 3D finite model of connection elements. The study is conducted on a simple small frame. First, a 3D model is constructed, followed by the construction of an equivalent 2D one. Firstly, we start with the static analysis; the results of the many proposed 1D element models are compared with the results of the 2D model. Secondly, we perform a dynamic analysis of the frame. It will be shown that with a special treatment of the connection elements, the results of the static and the dynamic analyses of the new 1D finite element model agree well with the results of the 2D model. i.e. with the 3D model.

Keywords: Structures, Finite element methods, Condensation, modal analysis, Timoshenko beam, Connection element, and Small frames.

Notations

E	Young's elastic modulus
ν	Poisson coefficient
ρ	density
I	moment of inertia
t	frame thickness
$\mathbf{k}(n,n)$	stiffness matrix of order n
$\mathbf{m}(n,n)$	mass matrix of order n
$\mathbf{L}(n,m)$	rectangular matrix with n rows and m columns
DOF	degree-of-freedom

1. INTRODUCTION

To perform a static and dynamic analysis of a 3D frame, 3-D finite elements are usually used in the meshing process. A large number of elements are required, which in turn requires a large number of DOF and consequently, a great deal of work. The main objective consists of developing a 1-D model made up of simple 1-D elements to replace the 3-D model made up of tetrahedral prisms or brick elements. To perform a static or a dynamic analysis, the calculation of the stiffness matrix and the mass matrix is required.

In order to find the best 1-D finite meshing element, 3-D meshing is used, then a 2-D and 1-D models are constructed at a later stage.

All calculations are performed using ANSYS®16.2 and MATLAB® 2016. A simple 3D frame is used in the calculations.

2. TEST STRUCTURE

Our test structure have the following simple form:

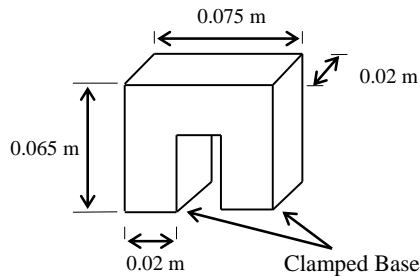


Figure 1: Test structure

The section of the horizontal beam and of the vertical column is rectangular ($0.02 \times 0.02 \text{ m}^2$). The mechanical characteristics of the material used are: Poisson coefficient $\nu = 0.31$, density $\rho = 78 \text{ KN/m}^3$, and elastic modulus $E = 184,000 \text{ KPa}$. Different types of elements are used in the meshing processes. At first stage the static analysis is performed, where the comparison between different models is based on the deformation in the XY plan of the structure as well as the plan perpendicular to the XY plan. These models are compared in 2 load cases illustrated in Figure 2:

- Case 1: a body load of 78000 N/m^3 along the vertical axis of the horizontal beam
- Case 2: a body load of 78000 N/m^3 along the horizontal axis of the left column

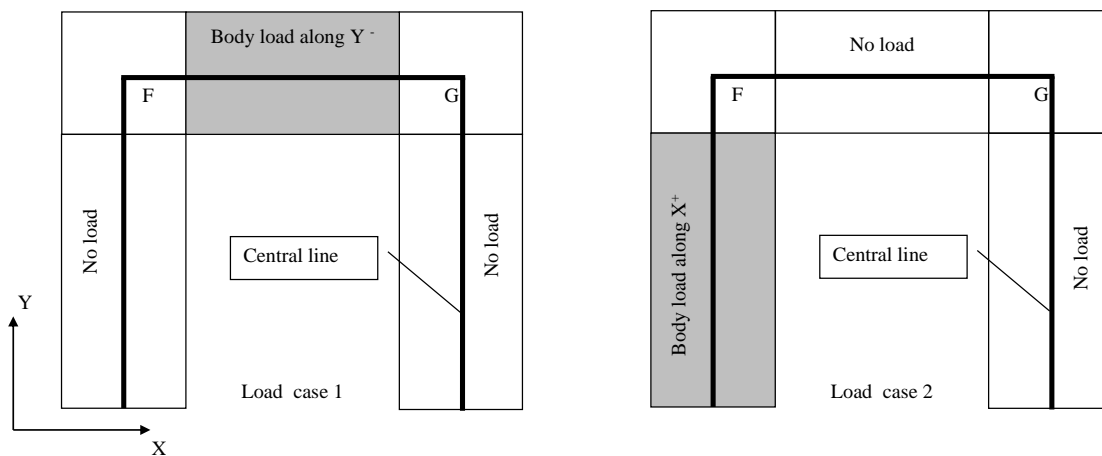


Figure 2: Test structure with load cases 1 and 2

Then, at a second stage; we will perform the dynamic analysis where we compare all results from all models with the result from the volumetric meshing model using brick finite element H8.

3. STATIC ANALYSIS

3.1 3D and 2D modeling

The 3D model of the test structure is meshed using H8 volumetric finite elements with 8 nodes.

Figures 5 and 6 show the total displacement contours of the frame under load case 1 and 2.

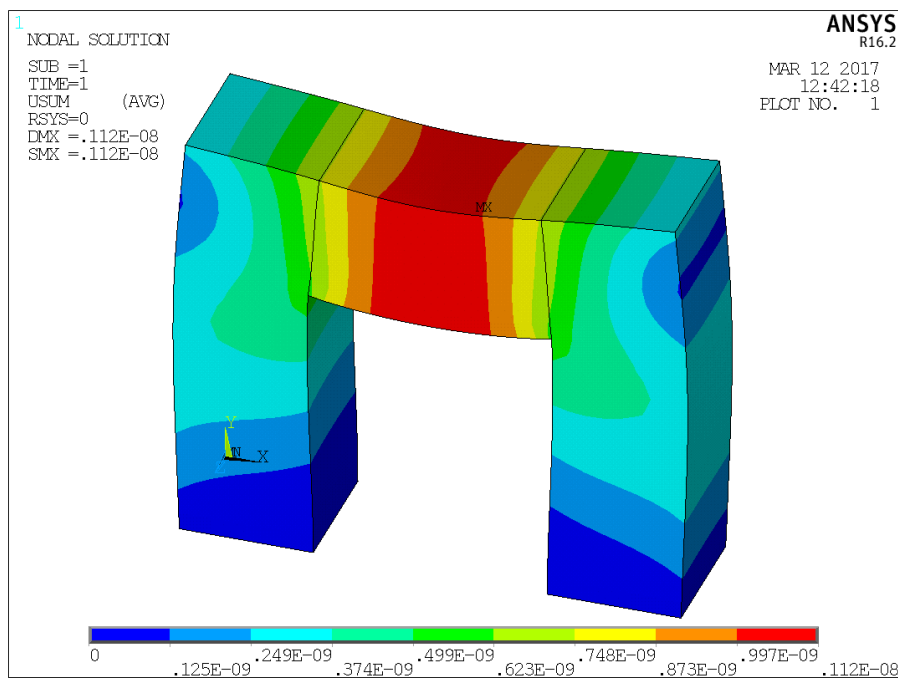


Figure 3: Three-dimensional deformed test structure under load case 1

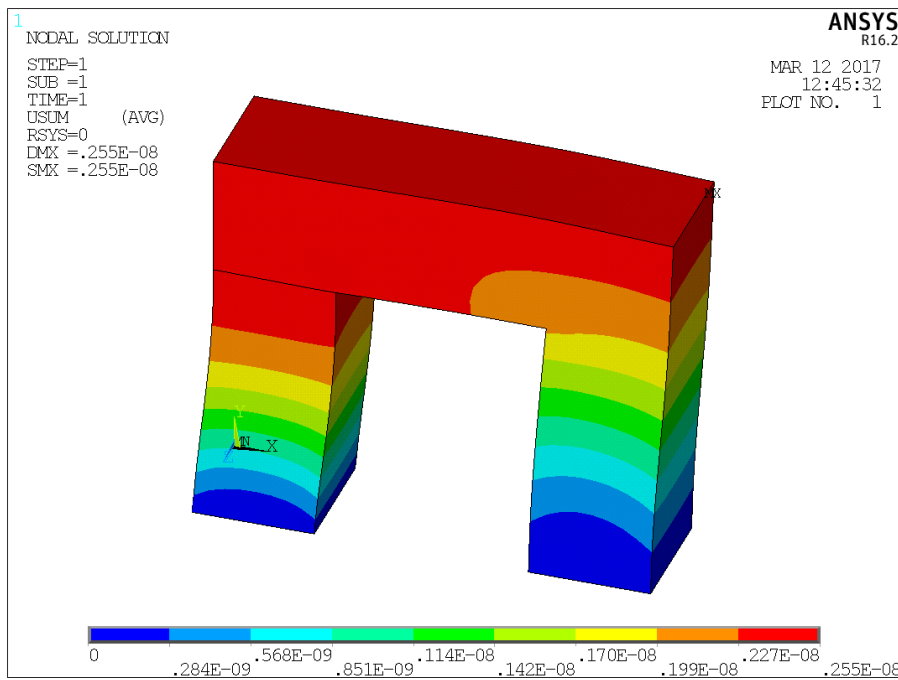


Figure 4: Three-dimensional deformed test structure under load case 2

The test structure is then modeled in two dimensions. A Q4 plane element with a thickness $t = 0.02$ m and having 4 nodes is used.

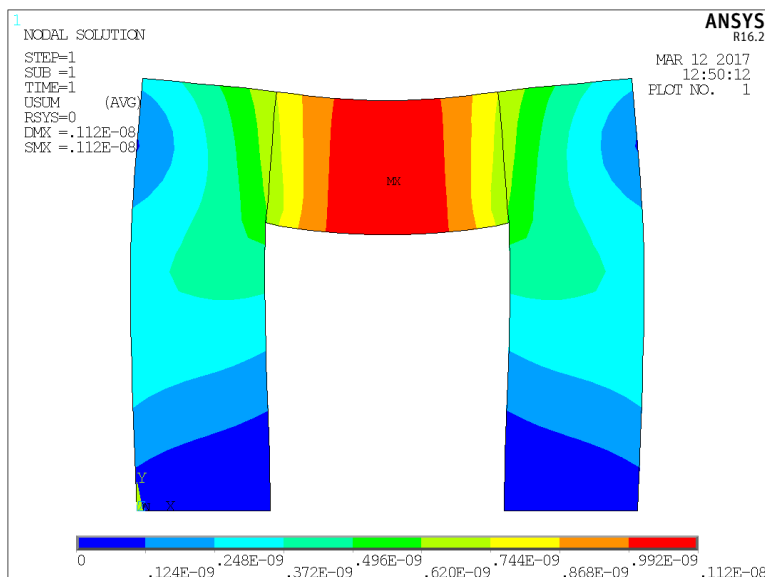


Figure 5: Two-dimensional deformed test structure along load case 1

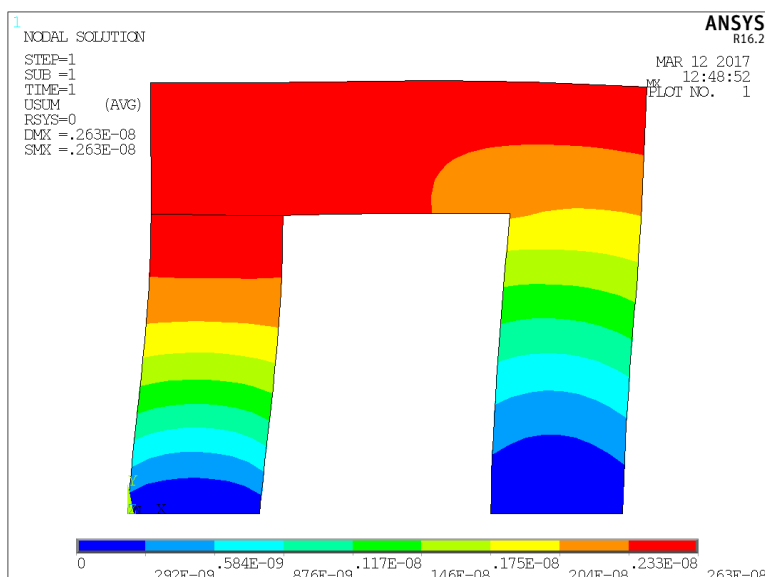


Figure 6: Two-dimensional deformed test structure along load case 2

Figures 4 and 5 have similar maps as Figures 5 and 6. The different models are compared using the displacement of 65 points on the central line of the longitudinal symmetrical plan of the structure.

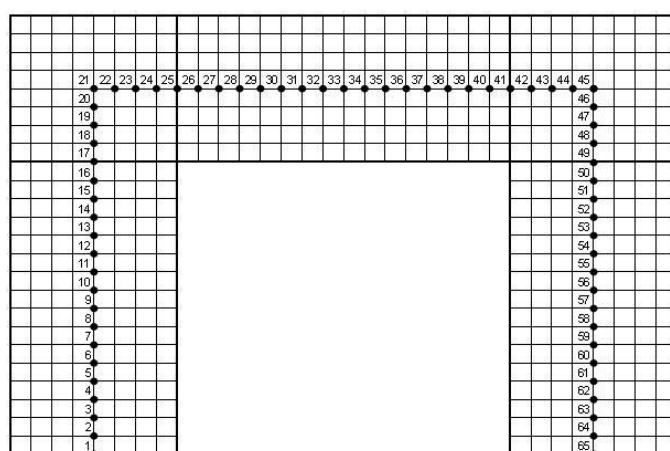


Figure 7 : Longitudinal symmetrical plan of the structure showing the 65 central line points

In order to establish a comparison between both FE models and using both load cases, UX and UY displacements of nodes on the central line, along the X and Y axis respectively, are plotted on the same graph (see Figure 8 – 10).

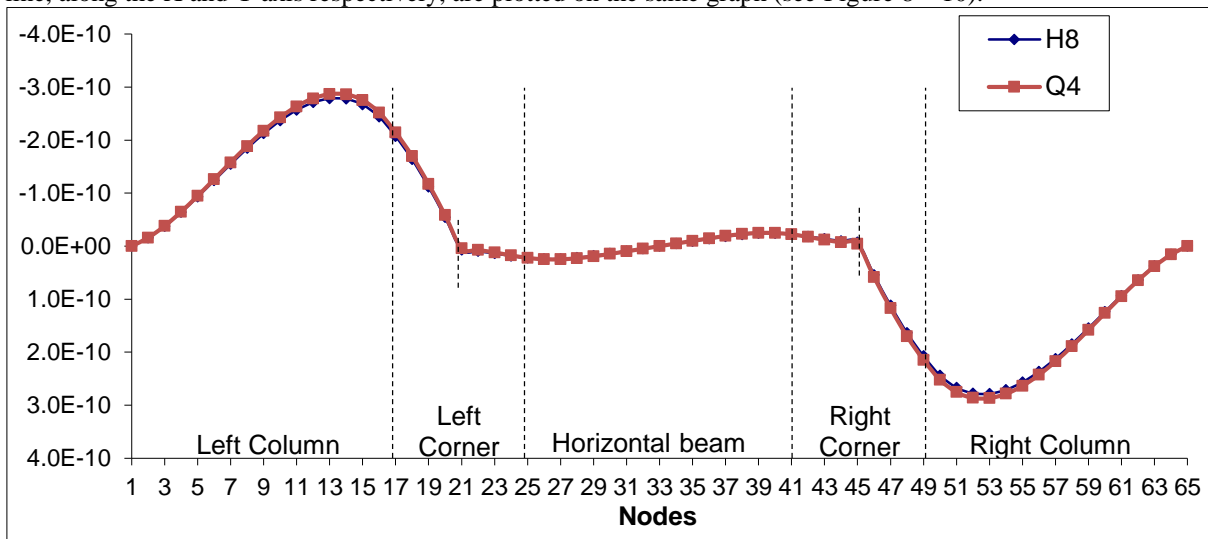


Figure 8 : UX (m) central line displacement along axe X (load case 1)

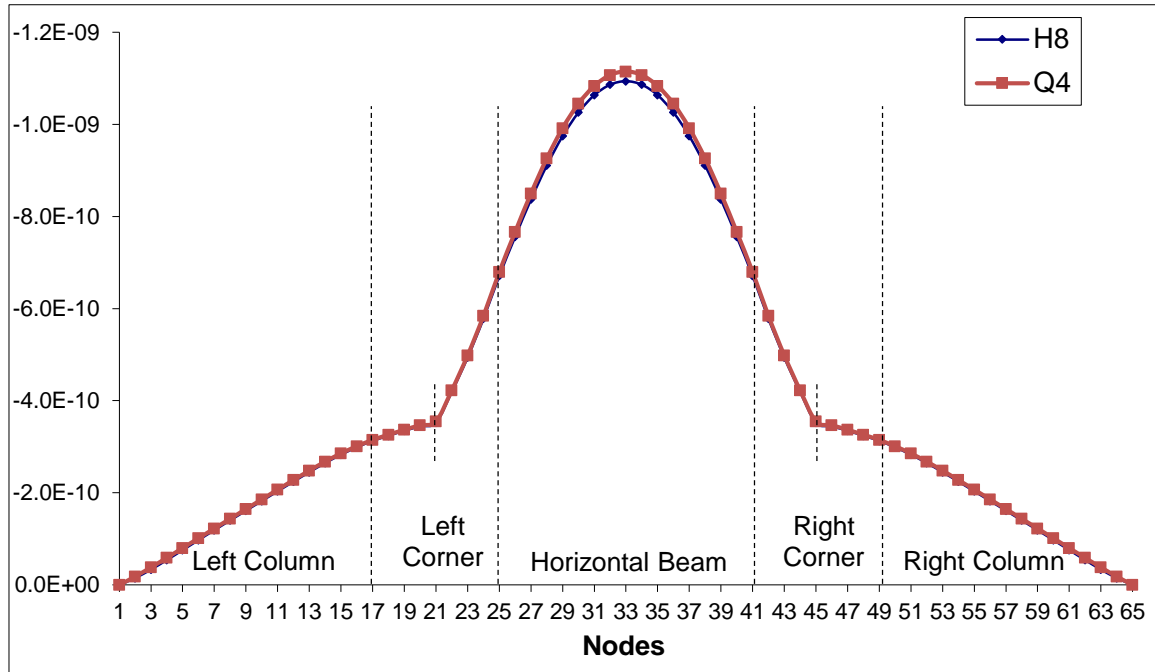


Figure 9 : UY (m) central line displacement along axe Y (load case 1)

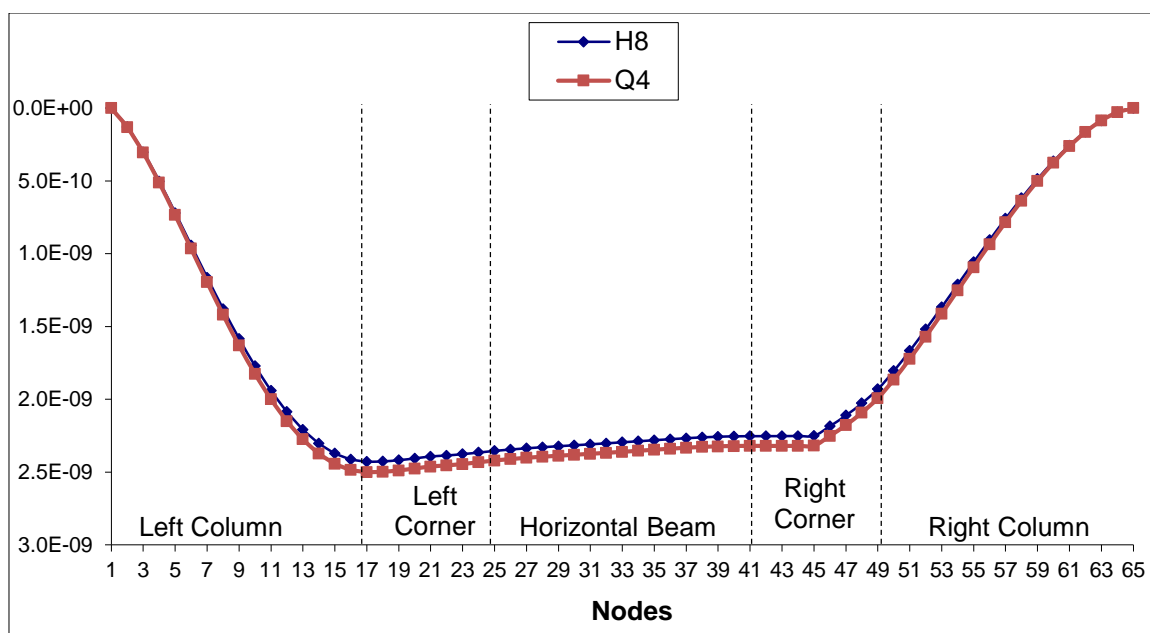


Figure 10 : UX (m) central line displacement along axe X (load case 2)

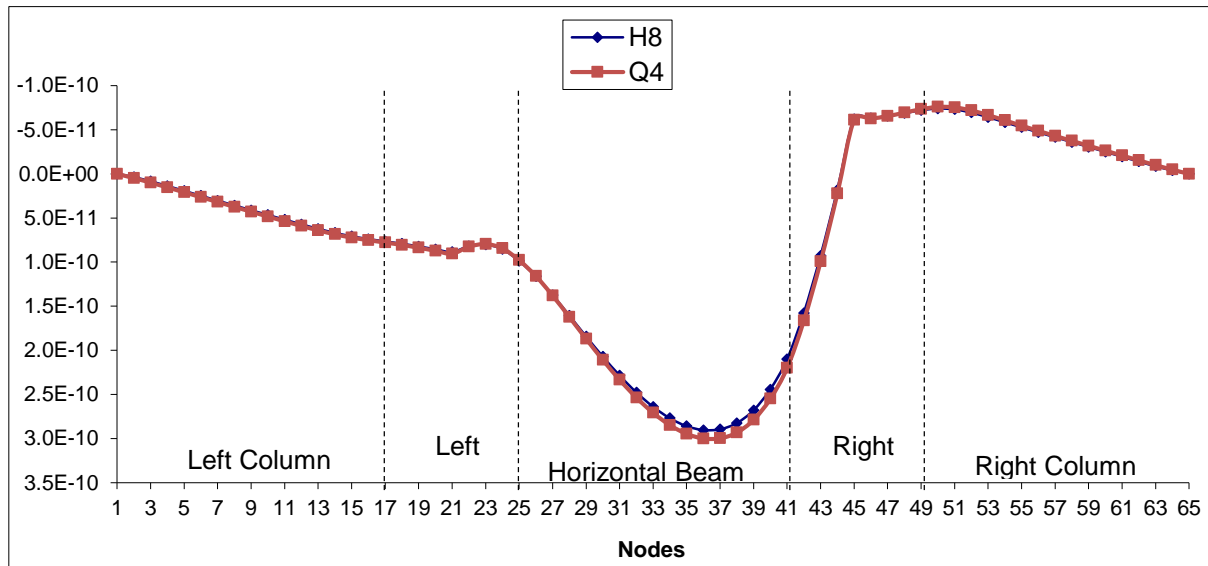


Figure 11 : UY (m) central line displacement along axe Y (load case 2)

Regarding the comparison criteria of the results produced by different models, the following error formula is used:

$$E_{\max} = \max_i \frac{|U_R(i) - U_C(i)|}{\max_j |U_R(j) - \min_j U_R(j)|}$$

$U_R(i)$ = reference value of a displacement at point i

$U_C(i)$ = calculated value of the same displacement and at the same point i of a new model

The maximum errors for both models H8 and Q4, for both load cases, are listed in Table 1 below:

Load case	Displacement	U_R (m) [H8]	U_C (m) [Q4]	E_{\max}	Node number (E_{\max})
1	UX	-2.6673E-10	-2.7536E-10	1.55%	15 and 51
1	UY	-1.0941E-09	-1.1149E-09	1.90%	33
2	UX	2.4111E-09	2.4842E-09	3.01%	16
2	UY	2.6802E-10	2.7866E-10	2.92%	39

Table 1: Comparison between H8 and Q4 models

The plane model has produced comparable results to those of the 3-D model. Thus, the reference model is the 2-D model which leads to a reduction in the DOF amount. It will be used to develop the best 1-D element for connection modeling.

3.2 One-dimensional classical modeling

In this section, 1-D elements are used for the test structure. Since the structure is not the slender type, we know that Euler-Bernoulli beams are not adequate. Therefore, we will use Timoshenko beams with 2 nodes per element and 3 DOF per node (Timoshenko model).

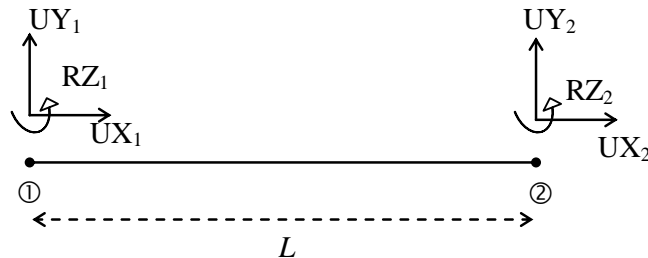


Figure 12 : Two-node beams

The transformation from the Q4 model to the 1-D model is shown in Figures 12 and 13. The volumetric charge is transformed into linear charge.

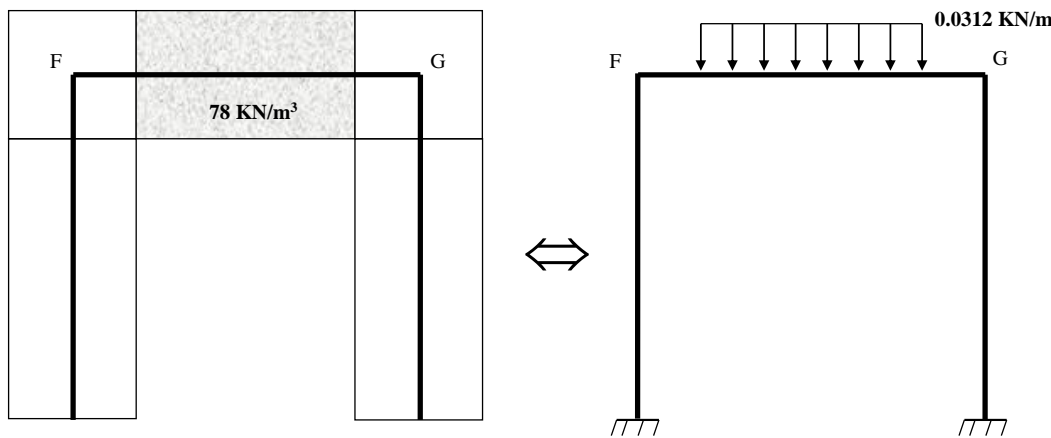


Figure 13 : Transformation of the Q4 model into a 1-D model (load case 1)

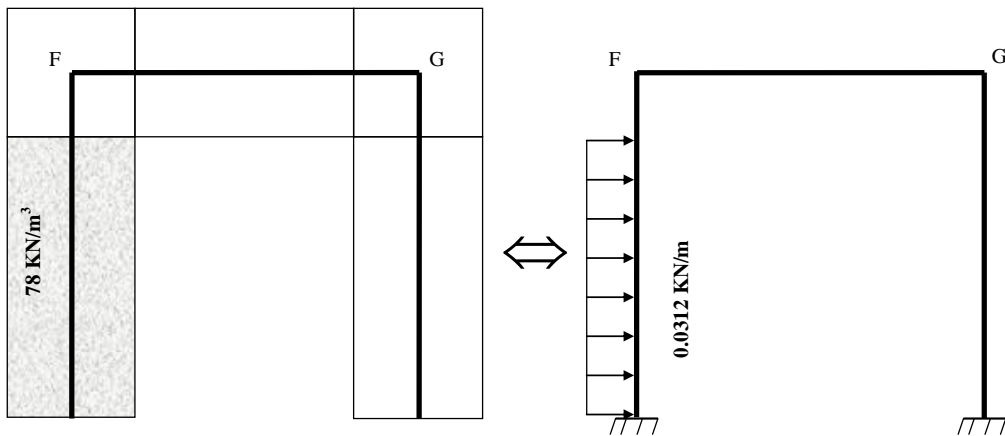


Figure 14 : Transformation of the Q4 model into a 1-D model (load case 2)

The left and right columns are modeled using 16 elements each. The horizontal beam is also modeled using 16 elements. Both left and right corners are modeled using 4 horizontal linear elements and 4 vertical linear elements, i.e. a total of 64 beam elements. The following figures show the deformed test structure in the 2 load cases as applicable to both models: the reference model Q4 and the Timoshenko model.

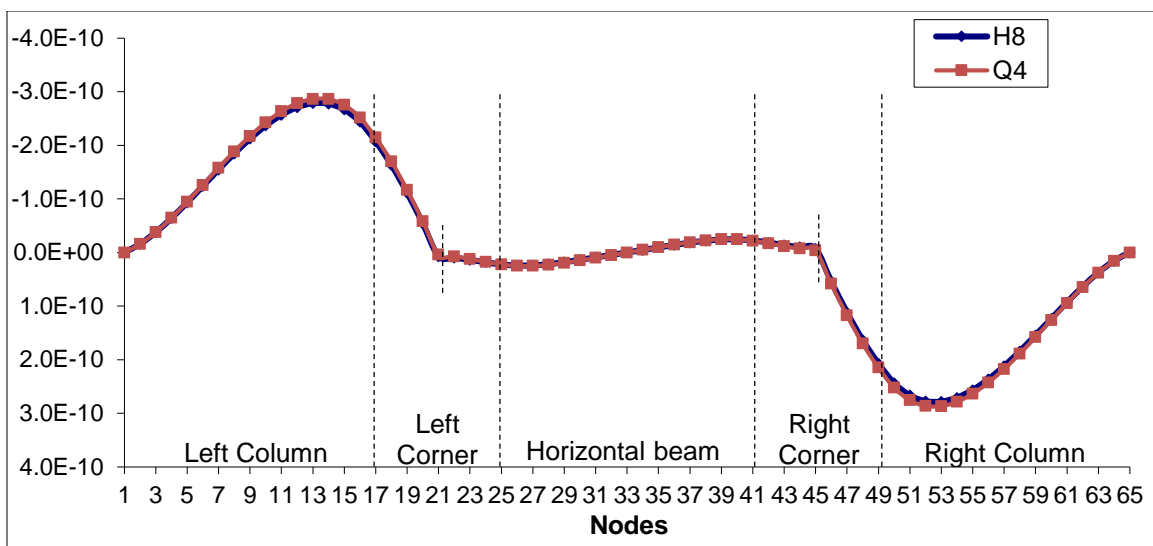


Figure 15 : UX (m) displacement of central line nodes along X (load case 1)

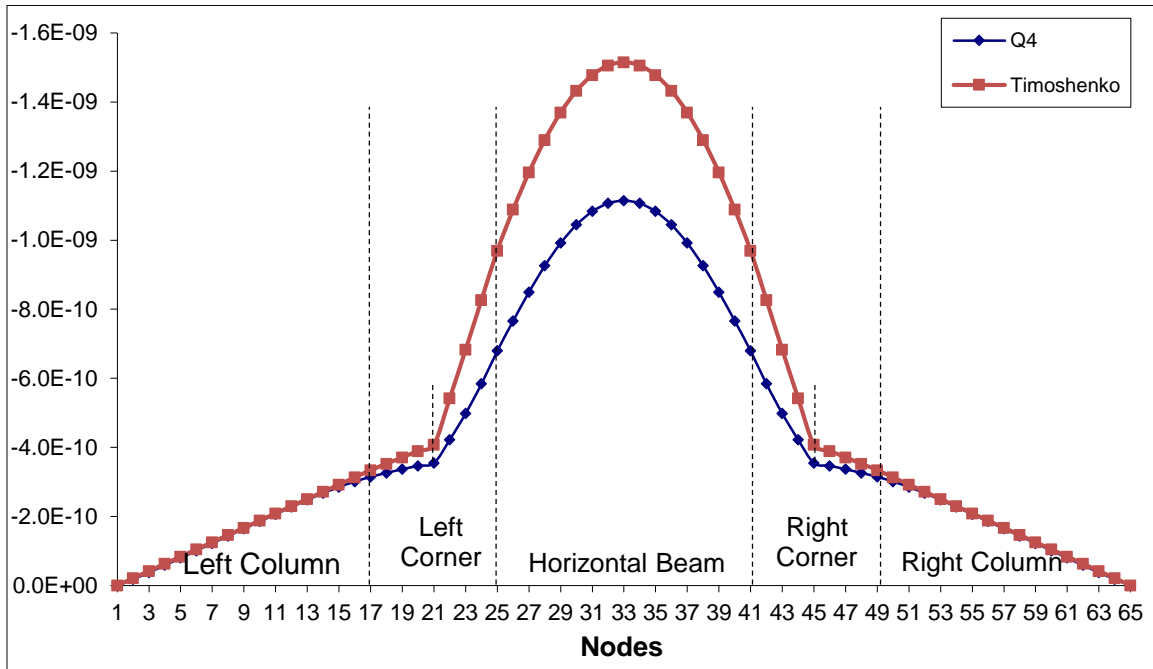


Figure 16 : UY (m) displacement of central line nodes along Y (load case 1)

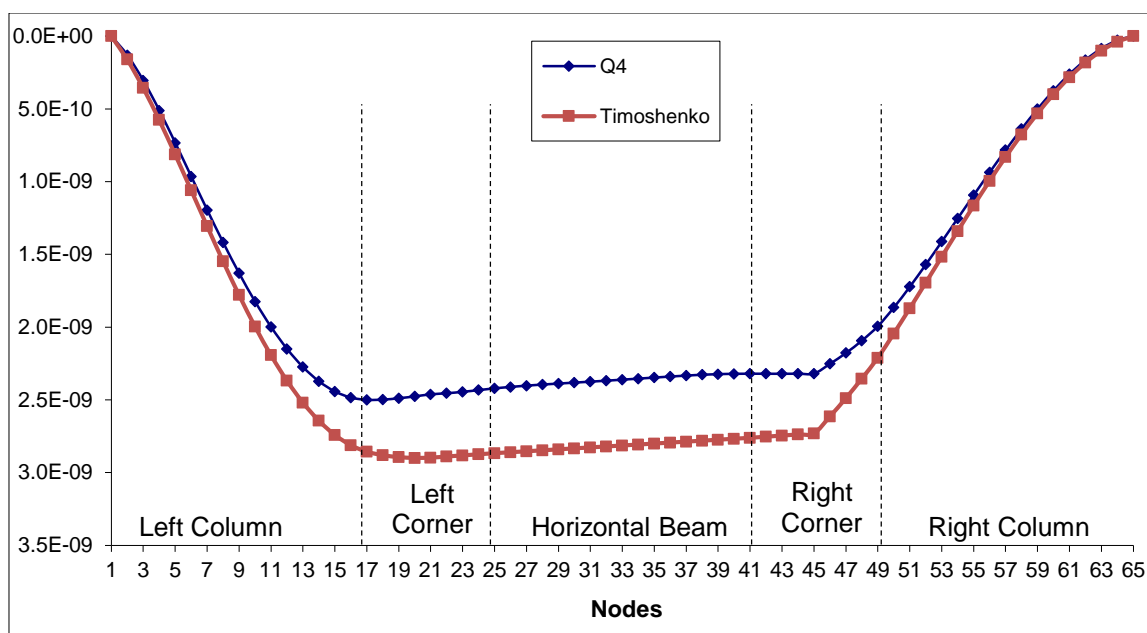


Figure 17 : UX (m) displacement of central line nodes X (load case 2)

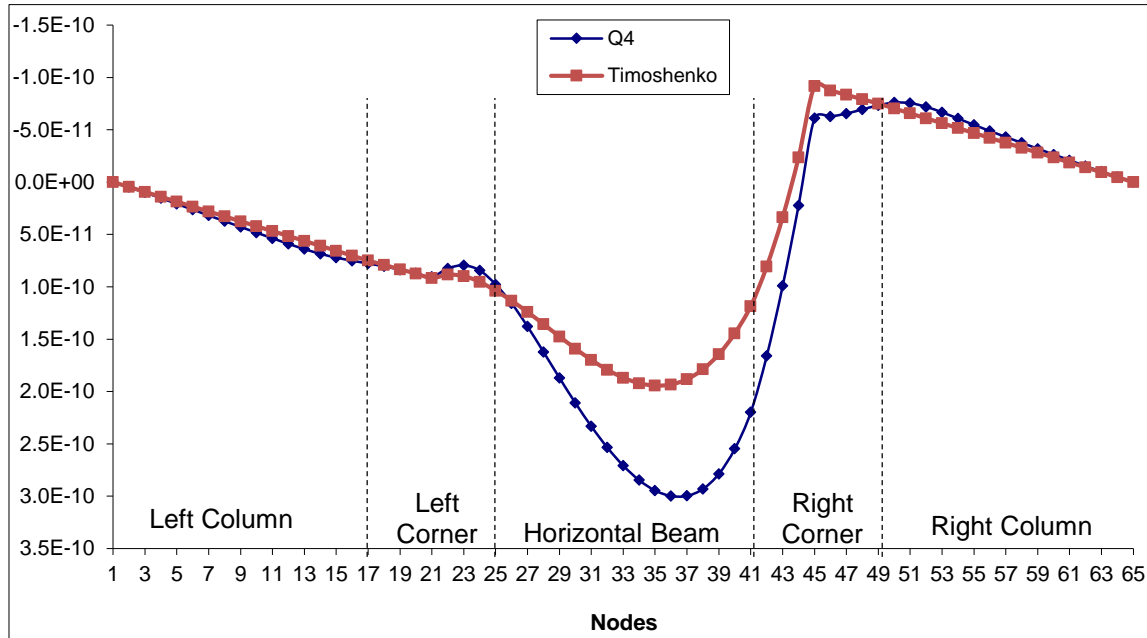


Figure 18 : UY (m) displacement of central line nodes Y (load case 2)

None of the 1-D models produces proximate results in comparison with those given by the Q4 model. Improved models using Timoshenko beams are shown below.

3.3 First improved model: CQ corner quad

A new CQ element is suggested for the corners, based on the utilization of Q4 surface elements since the Q4 modeling and the H8 modeling produce close results. Non-corner elements are still modeled as Timoshenko beams. One way to connect two different meshing types is explained by Dohrmann and al, [4] and [5], and Quiroz and al [9]. Kattner and al [8] explain how modeling joints between frame columns and beams is performed.

The interface between the new CQ element on the one hand and the horizontal and vertical beams on the other hand, is considered rigid in our case. The corner element of $0.02 \text{ m} \times 0.02 \text{ m}$ and 0.02 m in thickness is meshed using Q4 elements of $0.02/8 \text{ m} \times 0.02/8 \text{ m}$ which produces 64 elements and 81 nodes in total, hence 81×2 DOF: 17×2 interface DOF and 64×2 non-interface DOF (see next Figure).

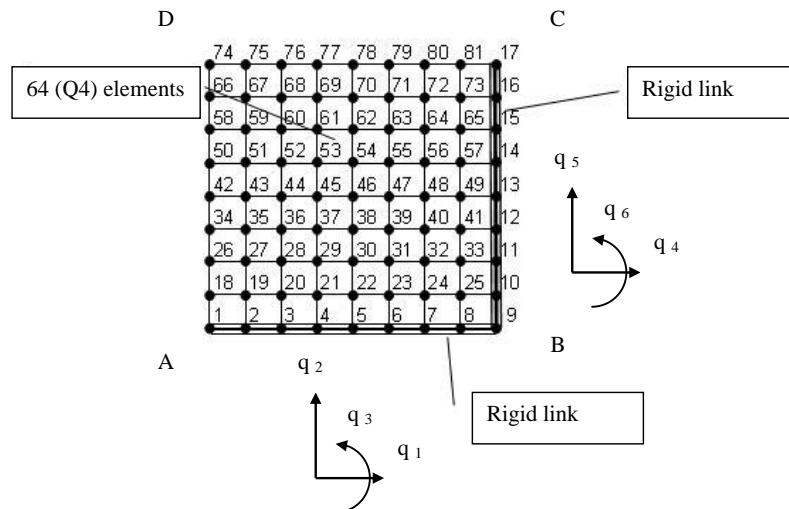


Figure 19 : Left corner with rigid links

The elementary stiffness matrix $k_e(8,8)$ of the Q4 element is mentioned in Cook [2]. By assembling the 64 Q4 elements, the global stiffness matrix of the corner is $K(162,162)$.

Using static condensation, the global stiffness matrix is reduced to $K_c(34,34)$ after elimination of the 128 non-interface DOF [3].

To find matrix $K_c(34,34)$, we use the formula for static condensation. In Matlab code:

```
krr=K(1:34,1:34);
krc=K(1:34,35:162);
kcr=K(35:162,1:34);
kcc=K(35:162,35:162);
Kc=krr-krc*inv(kcc)*kcr;
```

The AB interface is supposed to be rigid. Then, 3 DOF (q_1, q_2, q_3) are enough to determine the DOF of the AB interface:

- q_1 : horizontal displacement of the midpoint of segment AB
- q_2 : vertical displacement of the midpoint of segment AB
- q_3 : rotation of segment AB around its midpoint

The same applies to the BC interface where the DOF (q_4, q_5, q_6) of the midpoint in BC determine the DOF of the rigid interface BC.

The reduced stiffness matrix $K_r(6,6)$ is given by: $K_r = L^T K_c L$, where $L(34 \times 6)$ is the matrix giving the values of the DOF relative to interfaces AB and BC, from degrees q_1, q_2, q_3, q_4, q_5 , and q_6 .

$$L = \begin{bmatrix} 1 & 0 & 0 & 0 & 0 \\ 0 & 1 & -4*a & 0 & 0 \\ 1 & 0 & 0 & 0 & 0 \\ 0 & 1 & -3*a & 0 & 0 \\ 1 & 0 & 0 & 0 & 0 \\ 0 & 1 & -2*a & 0 & 0 \\ 1 & 0 & 0 & 0 & 0 \\ 0 & 1 & -1*a & 0 & 0 \\ 1 & 0 & 0 & 0 & 0 \\ 0 & 1 & 0 & 0 & 0 \\ 1 & 0 & 0 & 0 & 0 \\ 0 & 1 & 0 & 0 & 0 \\ 1 & 0 & 0 & 0 & 0 \\ 0 & 1 & 1*a & 0 & 0 \\ 1 & 0 & 0 & 0 & 0 \\ 0 & 1 & 2*a & 0 & 0 \\ 1 & 0 & 0 & 0 & 0 \\ 0 & 1 & 3*a & 0 & 0 \\ 0 & 0 & 0 & 1 & 0 \\ 0 & 1 & 4*a & 0 & 0 \\ 0 & 0 & 0 & 1 & 0 \\ 0 & 0 & 0 & 0 & 1 \end{bmatrix}$$

```

0 0 0 1 0 2*b
0 0 0 0 1 0
0 0 0 1 0 1*b
0 0 0 0 1 0
0 0 0 1 0 0
0 0 0 0 1 0
0 0 0 0 1 0
0 0 0 1 0 -1*b
0 0 0 0 1 0
0 0 0 1 0 -2*b
0 0 0 0 1 0
0 0 0 1 0 -3*b
0 0 0 0 1 0
0 0 0 1 0 -4*b
0 0 0 0 1 0 ] ;

```

The stiffness matrix $K_r(6 \times 6)$ is a function of:

- The length a of side AB
- The length b of side BC
- The elastic modulus E of the material in part ABCD
- The Poisson coefficient ν
- The thickness of the frame t

The stiffness matrix of the left corner beam of the test structure is given numerically by:

```

kleft=[

4.6660e+009 1.5022e+009 -5.2058e+006 -4.6660e+009 -1.5022e+009 -2.6432e+007
1.5022e+009 4.6660e+009 2.6432e+007 -1.5022e+009 -4.6660e+009 5.2058e+006
-5.2058e+006 2.6432e+007 3.7398e+005 5.2058e+006 -2.6432e+007 -5.7599e+004
-4.6660e+009 -1.5022e+009 5.2058e+006 4.6660e+009 1.5022e+009 2.6432e+007
-1.5022e+009 -4.6660e+009 -2.6432e+007 1.5022e+009 4.6660e+009 -5.2058e+006
-2.6432e+007 5.2058e+006 -5.7599e+004 2.6432e+007 -5.2058e+006 3.7398e+005]

```

With a simple transformation, we can obtain the stiffness matrix of the right corner beam:

```

kright=[

4.6660e+009 -1.5022e+009 -5.2058e+006 -4.6660e+009 1.5022e+009 -2.6432e+007
-1.5022e+009 4.6660e+009 -2.6432e+007 1.5022e+009 -4.6660e+009 -5.2058e+006
-5.2058e+006 -2.6432e+007 3.7398e+005 5.2058e+006 2.6432e+007 -5.7599e+004
-4.6660e+009 1.5022e+009 5.2058e+006 4.6660e+009 -1.5022e+009 2.6432e+007
1.5022e+009 -4.6660e+009 2.6432e+007 -1.5022e+009 4.6660e+009 5.2058e+006
-2.6432e+007 -5.2058e+006 -5.7599e+004 2.6432e+007 5.2058e+006 3.7398e+005]

```

Finally, the CQ model of the constructed frame is as follows:

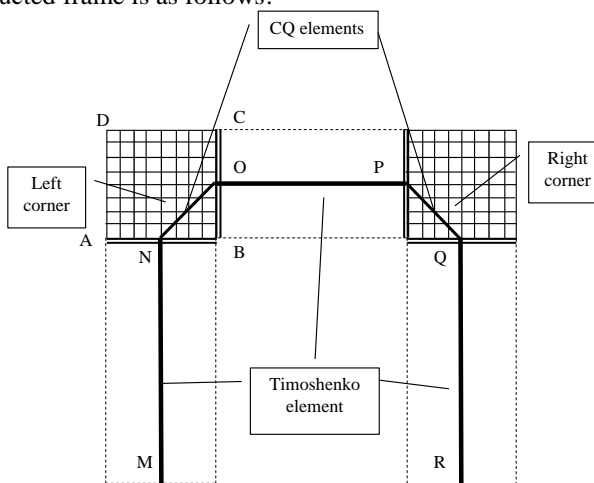


Figure 20 : Description of the CQ model

- MN, OP and QR are Timoshenko beams
 - NO is a CQ element with a $K_r \text{left}(6 \times 6)$ stiffness matrix
 - PQ is a CQ element with a $K_r \text{right}(6 \times 6)$ stiffness matrix
- Figures 24 to 27 show static results under load cases 1 and 2.

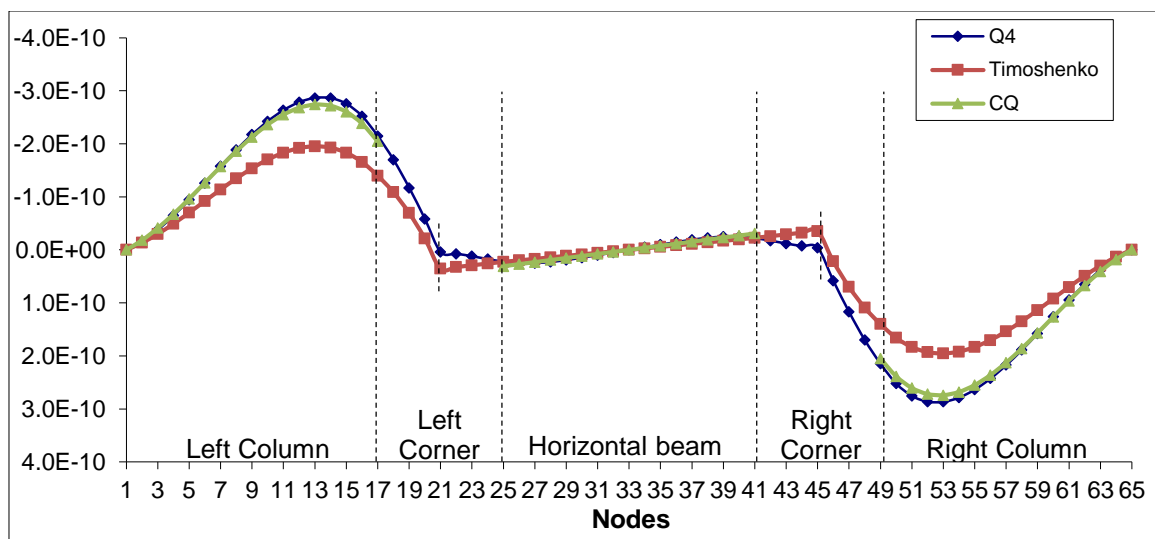


Figure 21 : UX (m) displacement of central line nodes along X (load case 1)

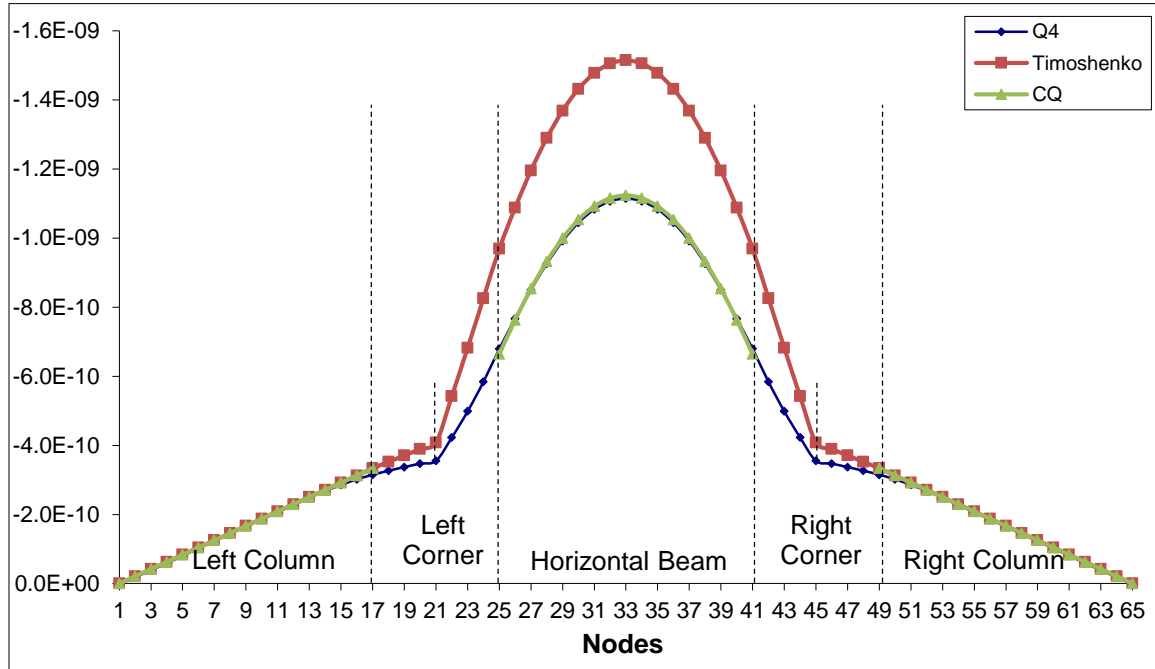


Figure 22 : UY (m) displacement of the central line nodes along Y (load case 1)

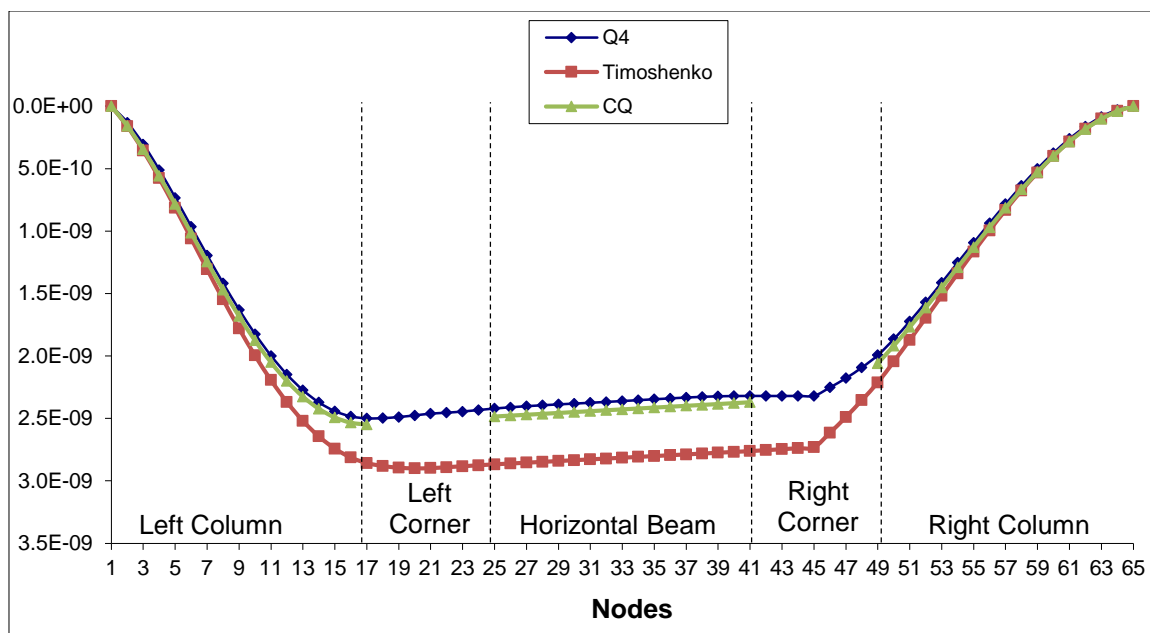


Figure 23 : UX (m) displacement of the central line nodes along X (load case 2)

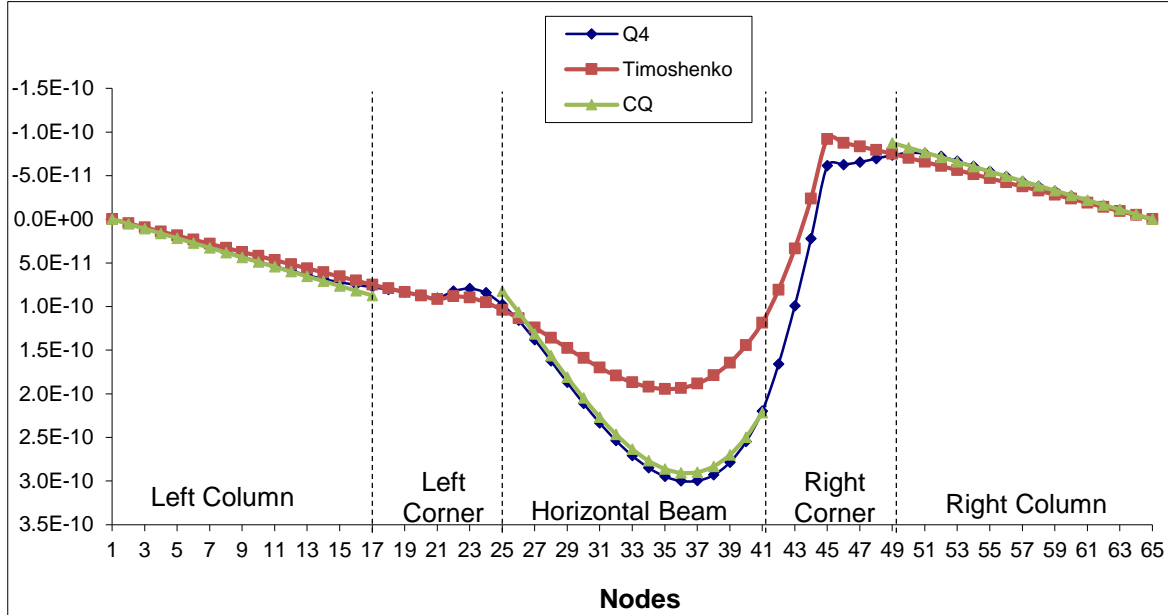


Figure 24 : UY (m) displacement of the central line nodes along Y (load case 2)

The graphs show that the results of the CQ model are very close to those of the Q4 model. Table 2 shows the results of both models for both load cases. The last column gives the node number corresponding to the highest error value E_{max} .

Load case	Displacement	U_R (m) [Q4]	Model	U_C (m)	E_{max}	Node number (E_{max})
1	UX	2.8613E-10	Timoshenko	1.9284E-10	16.28%	14 or 52
1	UY	-1.1149E-09	Timoshenko	-1.5148E-09	35.87%	33
2	UX	2.3397E-09	Timoshenko	2.7944E-09	18.19%	36 or 37
2	UY	2.7866E-10	Timoshenko	1.645E-10	30.38%	39
1	UX	-2.7536E-10	CQ	-2.6053E-10	2.59%	15 or 51
1	UY	-3.1495E-10	CQ	-3.3374E-10	1.69%	17 or 49
2	UX	2.3947E-09	CQ	2.4623E-09	2.70%	28
2	UY	9.7806E-11	CQ	8.2391E-11	4.10%	25

Table 2 : Comparison of both models and all load cases

It can be said from the previous table, that the CQ model produces the best approximation to the Q4 model.

3.4 Second improved model: Rigid interface everywhere (RQ)

In this paragraph, we propose a linear finite element to replace Timoshenko beams in the vertical and horizontal beams. This new element is constructed using the same procedure for the corner elements as in the previous paragraph.

Consider a strip in the beam that is between two consecutive nodes of the midline (see next figure).

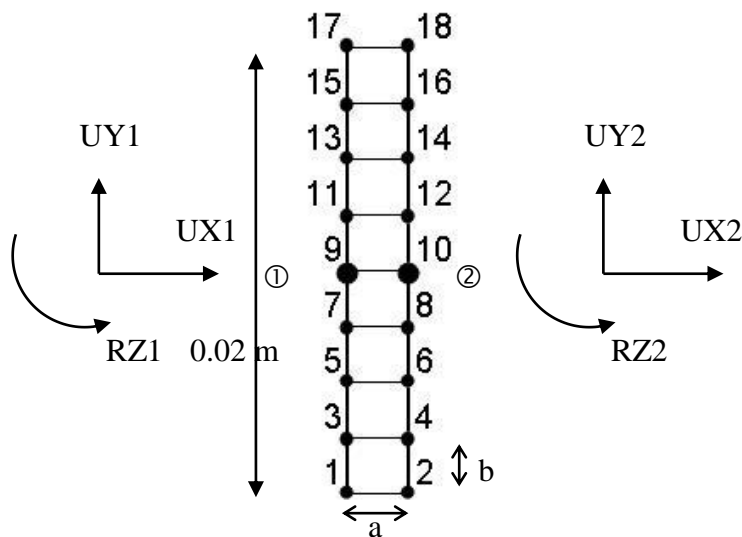
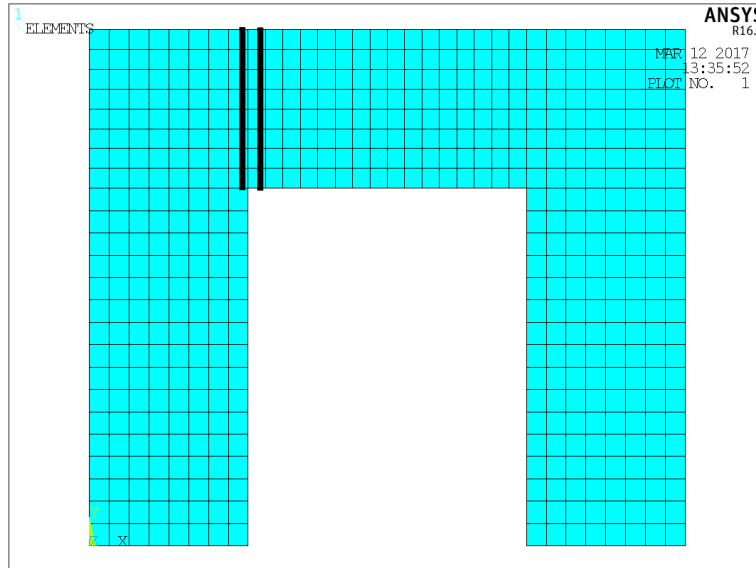


Figure 25: RQ element

The total length of this element is 0.02 m (from bottom to top). The thickness (along z direction) is always 0.02 m. $a = b = 0.045/16 = 0.0028125$ m.

The element is discretized in 8 Q4 elements along its length. Therefore, we have a total of 9 nodes and 18 DOF for each interface.

We will assume that plane sections of beams in bending (Timoshenko hypothesis), displacements of nodes that are in the same cut-section are displacements of a rigid body, given by 3 DOFs:

- UX = Displacement along the X axis of the center of the section
- UY = Displacement along the Y axis of the center of the section
- RZ = Rotation around the Z axis

Therefore, the displacements of all the nodes of this element are given by 6 DOFs; 3 DOFs for the left cut-section and 3 DOFs for the right cut-section. This will give us the elementary stiffness matrix $ke(6,6)$. In order to determine $ke(6,6)$, we know that the stiffness matrix for one Q4 element is given by:

The global matrix is K(36,36).

The matrix of the rigid interface is given by:

```
R=[  
 1 0 4*b 0 0 0  
 0 1 0 0 0 0  
 0 0 0 1 0 4*b  
 0 0 0 0 1 0  
 1 0 3*b 0 0 0  
 0 1 0 0 0 0  
 0 0 0 1 0 3*b  
 0 0 0 0 1 0  
 1 0 2*b 0 0 0  
 0 1 0 0 0 0  
 0 0 0 1 0 2*b  
 0 0 0 0 1 0  
 1 0 1*b 0 0 0  
 0 1 0 0 0 0  
 0 0 0 1 0 1*b  
 0 0 0 0 1 0  
 1 0 0 0 0 0  
 0 1 0 0 0 0  
 0 0 0 1 0 0  
 0 0 0 0 1 0  
 1 0 -1*b 0 0 0  
 0 1 0 0 0 0  
 0 0 0 1 0 -1*b  
 0 0 0 0 1 0  
 1 0 -2*b 0 0 0  
 0 1 0 0 0 0  
 0 0 0 1 0 -2*b  
 0 0 0 0 1 0  
 1 0 -3*b 0 0 0  
 0 1 0 0 0 0  
 0 0 0 1 0 -3*b  
 0 0 0 0 1 0  
 1 0 -4*b 0 0 0  
 0 1 0 0 0 0  
 0 0 0 1 0 -4*b  
 0 0 0 0 1 0 ]
```

Therefore, $K = L^T \times K_c \times L$. (K_c is the condensed matrix). We obtain:

```
k=E*t/(v^2-1)*b/a*[  
-8, 0, 0, 0, 0, 0  
0, 4*v-4, 2*a*(v-1), 0, -4*v+4, 2*a*(v-1)  
0, 2*a*(v-1), -128/3*b^2-4/3*a^2+4/3*a^2*v, 0, -2*a*(v-1), 128/3*b^2-2/3*a^2+2/3*a^2*v  
8, 0, 0, -8, 0, 0  
0, -4*v+4, -2*a*(v-1), 0, 4*v-4, -2*a*(v-1)  
0, 2*a*(v-1), 128/3*b^2-2/3*a^2+2/3*a^2*v, 0, -2*a*(v-1), -128/3*b^2-4/3*a^2+4/3*a^2*v]
```

Our new modeling is shown in the next figure:

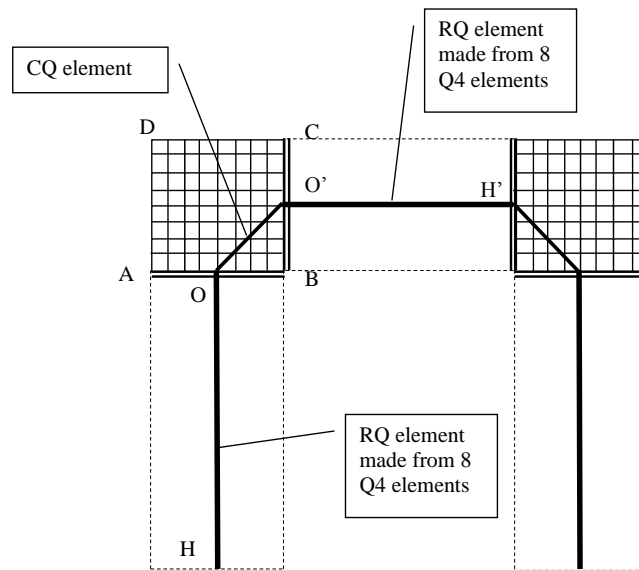


Figure 26: RQ model for the horizontal and vertical beams while CQ element at the corners

HO and O'H' are beam elements formed from 8 Q4 elements. OO' is a corner element.

The following graphs show the displacements along X and Y, for the two load cases for all the models that we have considered so far (Q4, Timoshenko, CQ, and RQ):

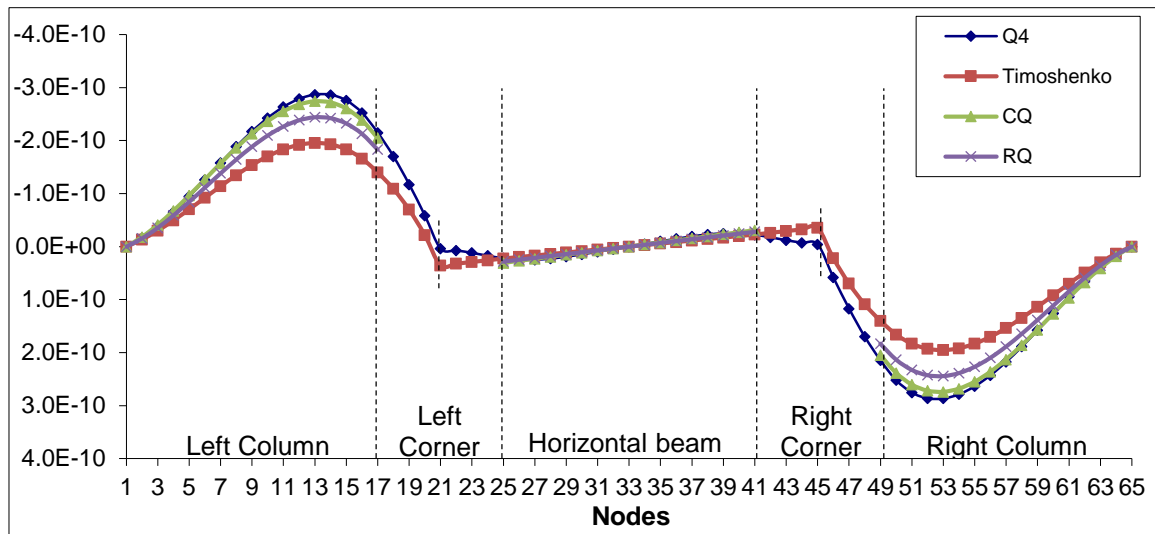


Figure 27 : UX (m) displacement of the central line nodes along X (load case 1)

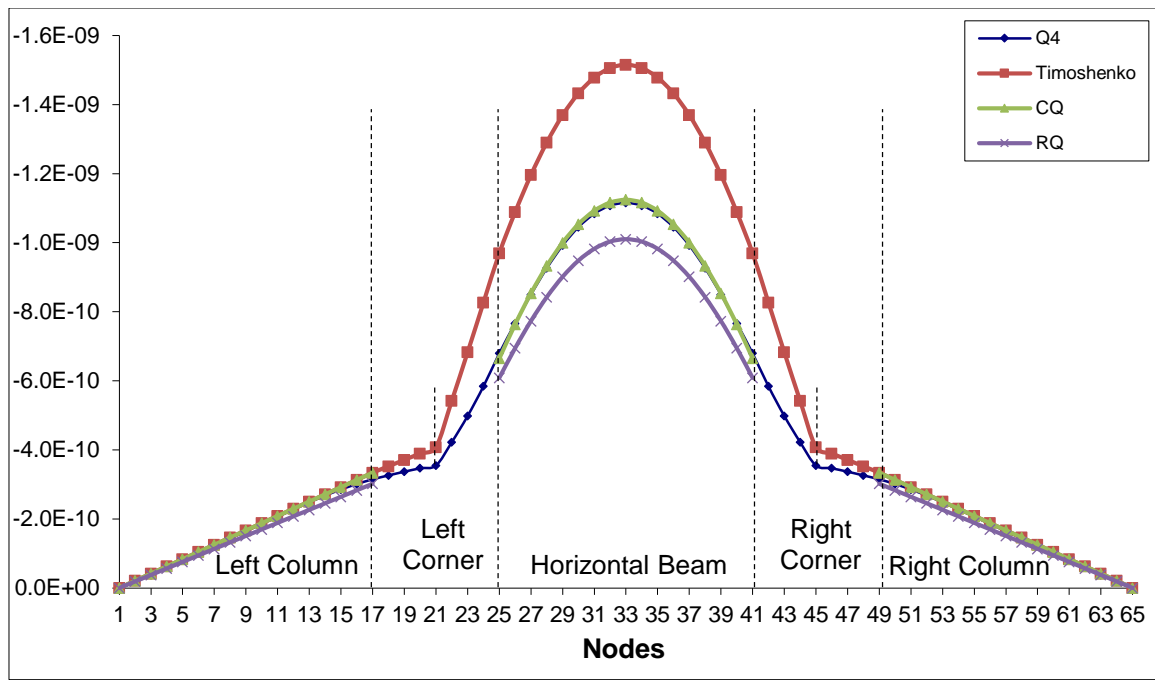


Figure 28 : UY (m) displacement of the central line nodes along Y (load case 1)

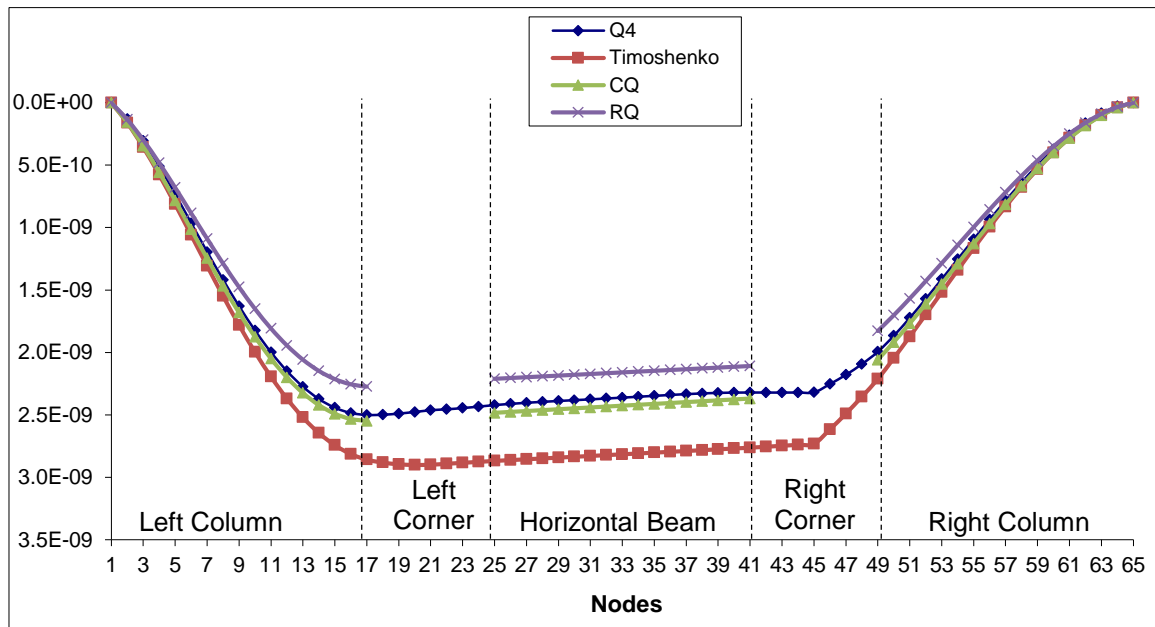


Figure 29: UX (m) displacement of the central line nodes along X (load case 2)

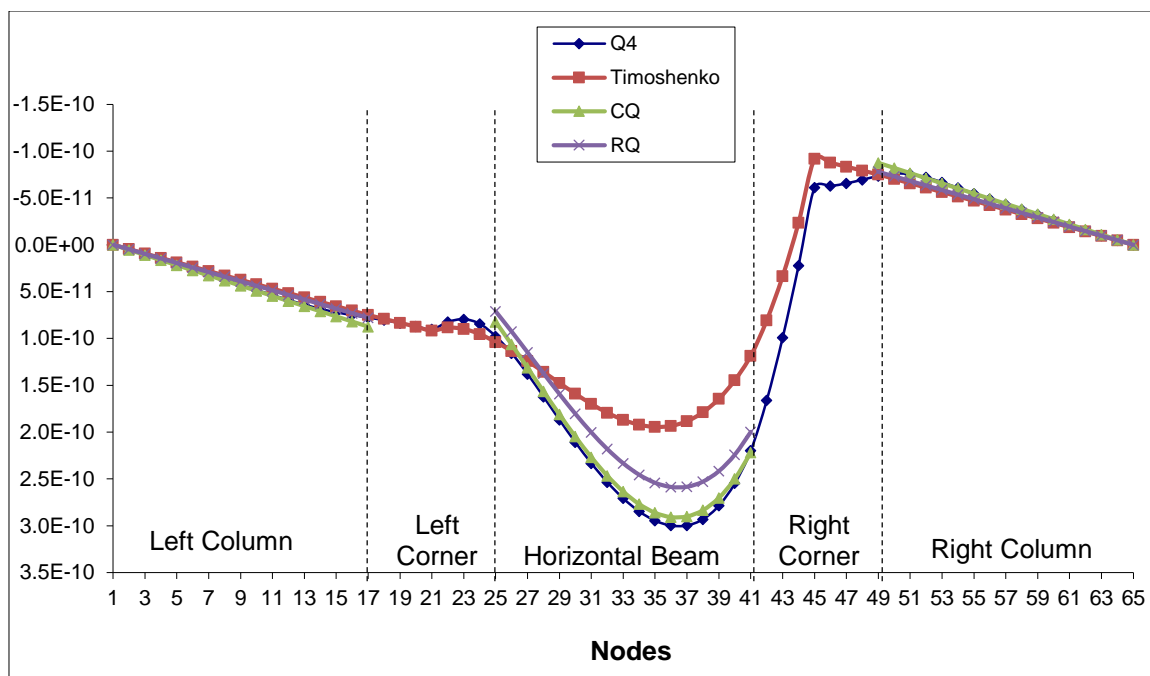


Figure 30 : UY (m) displacement of the central line nodes along Y (load case 2)

3.5 Third improved model (RQw)

The graphs of the previous paragraph show that the RQ model is a little stiffer than the CQ model. In order to give it a certain flexibility, we will add two DOFs (warping) for every node of the previous paragraph:

A new element is constructed from the RQ model that allows a plane section of a beam to deform a cubic or quadratic deformation after solicitation. Therefore, two DOFs will be added on each node:

A warping (in terms of y^2) that allows a quadratic displacement of the plane section and another warping term (in terms of y^3) that allows a cubic displacement of the plane section. The following figure illustrates the 5 DOFs on each node for the new element.

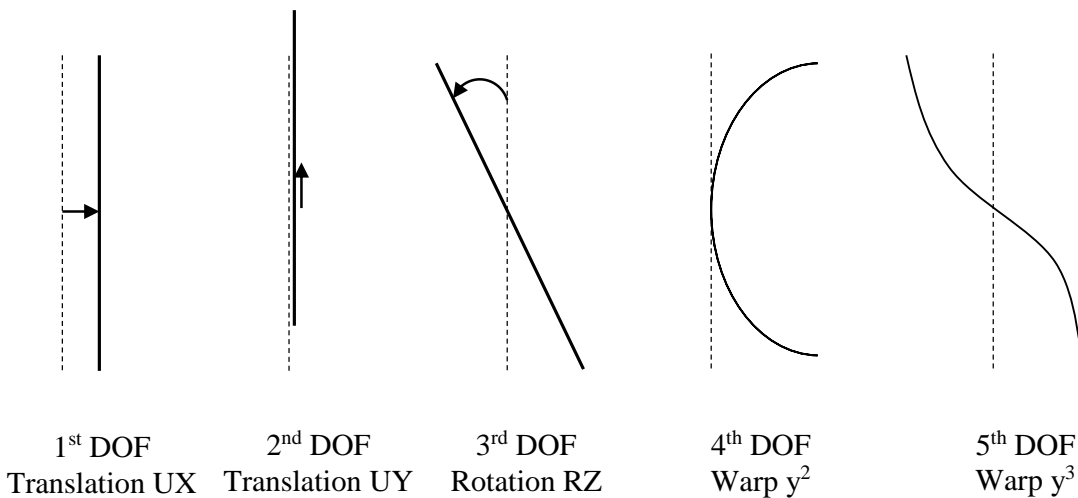


Figure 31: The 5 DOFs for the RQw model

For this element with 5 DOFs per node we expect a stiffness matrix k(10,10). The terms of the 4th and 5th degree of the stiffness degree are calculated as follows:

We find the global matrix K(36,36), then matrix L of the rigid link:

```
L=[ 1 0 4*b -16*b^2 64*b^3 0 0 0 0
0 1 0 0 0 0 0 0 0
0 0 0 0 0 1 0 4*b -16*b^2 64*b^3
0 0 0 0 0 0 1 0 0 0
1 0 3*b -9*b^2 27*b^3 0 0 0 0 0
0 1 0 0 0 0 0 0 0 0
0 0 0 0 0 1 0 3*b -9*b^2 27*b^3
0 0 0 0 0 0 1 0 0 0
1 0 2*b -4*b^2 8*b^3 0 0 0 0 0
0 1 0 0 0 0 0 0 0 0
0 0 0 0 0 1 0 2*b -4*b^2 8*b^3
0 0 0 0 0 0 1 0 0 0
1 0 1*b -1*b^2 1*b^3 0 0 0 0 0
0 1 0 0 0 0 0 0 0 0
0 0 0 0 0 1 0 1*b -1*b^2 1*b^3
0 0 0 0 0 0 1 0 0 0
1 0 0 0 0 0 0 0 0 0
0 1 0 0 0 0 0 0 0 0
0 0 0 0 0 1 0 0 0 0
0 0 0 0 0 0 1 0 0 0
1 0 -1*b -1*b^2 -1*b^3 0 0 0 0 0
0 1 0 0 0 0 0 0 0 0
0 0 0 0 0 1 0 0 0 0
0 0 0 0 0 0 1 0 0 0
1 0 -2*b -4*b^2 -8*b^3 0 0 0 0 0
0 1 0 0 0 0 0 0 0 0
0 0 0 0 0 1 0 0 0 0
0 0 0 0 0 0 1 0 0 0
1 0 -3*b -9*b^2 -27*b^3 0 0 0 0 0
0 1 0 0 0 0 0 0 0 0
0 0 0 0 0 1 0 0 0 0
0 0 0 0 0 0 1 0 0 0
1 0 -4*b -16*b^2 -64*b^3 0 0 0 0 0
0 1 0 0 0 0 0 0 0 0
0 0 0 0 0 1 0 0 0 0
0 0 0 0 0 0 1 0 0 0 ];
```

We can find:

$$k = L^T * K * L$$

the stiffness matrix k for the left corner with (warp) is given numerically by:

```
kleft =
4.6660e+009 1.5022e+009 -5.2058e+006 -7.3236e+004 -4.3907e+002 -4.6660e+009 -1.5022e+009 -2.6432e+007 2.5186e+005 -1.8964e+003
1.5022e+009 4.6660e+009 2.6432e+007 -2.5186e+005 1.8964e+003 -1.5022e+009 -4.6660e+009 5.2058e+006 7.3236e+004 4.3907e+002
-5.2058e+006 2.6432e+007 3.7398e+005 -1.6755e+003 2.7583e+001 5.2058e+006 -2.6432e+007 -5.7599e+004 -1.1072e+002 -4.2280e+000
-7.3236e+004 -2.5186e+005 -1.6755e+003 2.8150e+001 -1.2750e-001 7.3236e+004 2.5186e+005 -1.1072e+002 -4.7061e+000 8.7138e-005
-4.3907e+002 1.8964e+003 2.7583e+001 -1.2750e-001 2.6159e-003 4.3907e+002 -1.8964e+003 -4.2280e+000 8.7138e-005 -4.0191e-004
-4.6660e+009 -1.5022e+009 5.2058e+006 7.3236e+004 4.3907e+002 4.6660e+009 1.5022e+009 2.6432e+007 -2.5186e+005 1.8964e+003
-1.5022e+009 -4.6660e+009 -2.6432e+007 2.5186e+005 -1.8964e+003 1.5022e+009 4.6660e+009 -5.2058e+006 -7.3236e+004 -4.3907e+002
-2.6432e+007 5.2058e+006 -5.7599e+004 -1.1072e+002 -4.2280e+000 2.6432e+007 -5.2058e+006 3.7398e+005 -1.6755e+003 2.7583e+001
-2.5186e+005 7.3236e+004 -1.1072e+002 -4.7061e+000 8.7138e-005 -2.5186e+005 -7.3236e+004 -1.6755e+003 2.8150e+001 -1.2750e-001
-1.8964e+003 4.3907e+002 -4.2280e+000 8.7138e-005 -4.0191e-004 1.8964e+003 -4.3907e+002 2.7583e+001 -1.2750e-001 2.6159e-003
```

With a simple transformation, we can find the stiffness matrix of the right corner of our structure:

```
kright =
4.6660e+009 -1.5022e+009 -5.2058e+006 -7.3236e+004 -4.3907e+002 -4.6660e+009 1.5022e+009 -2.6432e+007 2.5186e+005 -1.8964e+003
-1.5022e+009 4.6660e+009 -2.6432e+007 2.5186e+005 -1.8964e+003 1.5022e+009 -4.6660e+009 -5.2058e+006 -7.3236e+004 -4.3907e+002
-5.2058e+006 -2.6432e+007 3.7398e+005 -1.6755e+003 2.7583e+001 5.2058e+006 -2.6432e+007 -5.7599e+004 -1.1072e+002 -4.2280e+000
-7.3236e+004 2.5186e+005 -1.6755e+003 2.8150e+001 -1.2750e-001 7.3236e+004 2.5186e+005 -1.1072e+002 -4.7061e+000 8.7138e-005
-4.3907e+002 -1.8964e+003 2.7583e+001 -1.2750e-001 2.6159e-003 4.3907e+002 1.8964e+003 -4.2280e+000 8.7138e-005 -4.0191e-004
-4.6660e+009 1.5022e+009 5.2058e+006 7.3236e+004 4.3907e+002 4.6660e+009 -1.5022e+009 2.6432e+007 -2.5186e+005 1.8964e+003
1.5022e+009 -4.6660e+009 2.6432e+007 -2.5186e+005 1.8964e+003 -1.5022e+009 4.6660e+009 5.2058e+006 7.3236e+004 4.3907e+002
-2.6432e+007 -5.2058e+006 -5.7599e+004 -1.1072e+002 -4.2280e+000 2.6432e+007 5.2058e+006 3.7398e+005 -1.6755e+003 2.7583e+001
-2.5186e+005 -7.3236e+004 -1.1072e+002 -4.7061e+000 8.7138e-005 -2.5186e+005 7.3236e+004 -1.6755e+003 2.8150e+001 -1.2750e-001
-1.8964e+003 -4.3907e+002 -4.2280e+000 8.7138e-005 -4.0191e-004 1.8964e+003 4.3907e+002 2.7583e+001 -1.2750e-001 2.6159e-003
```

The following figures show the displacements along X et Y, for both the load cases, for all models (Reference model: Q4 model, Timoshenko model, CQ model, RQ, model and RQw).

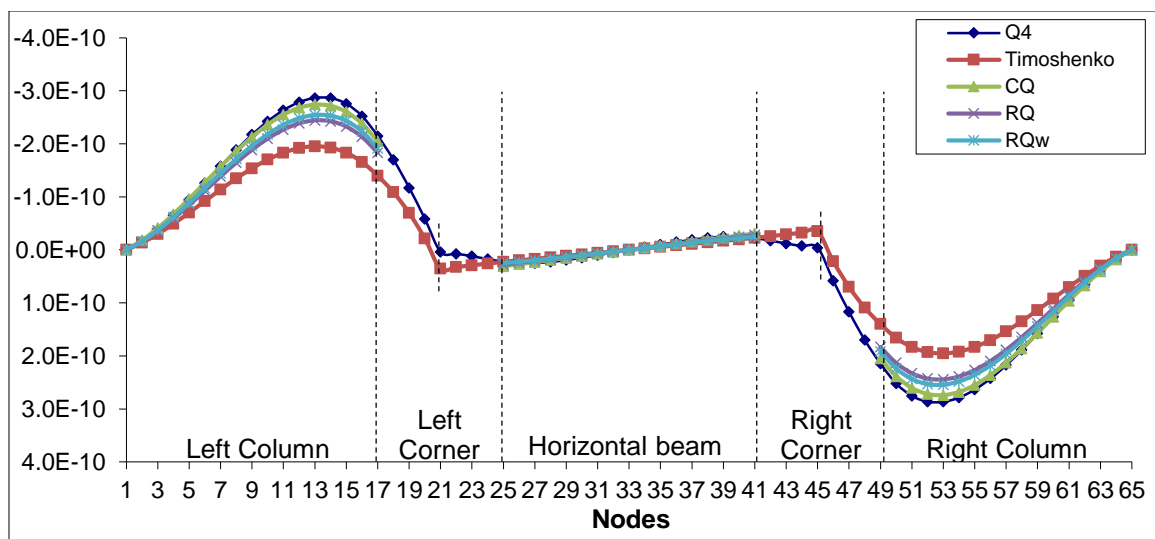


Figure 32: UX (m) displacement of the central line nodes along X (load case 1)

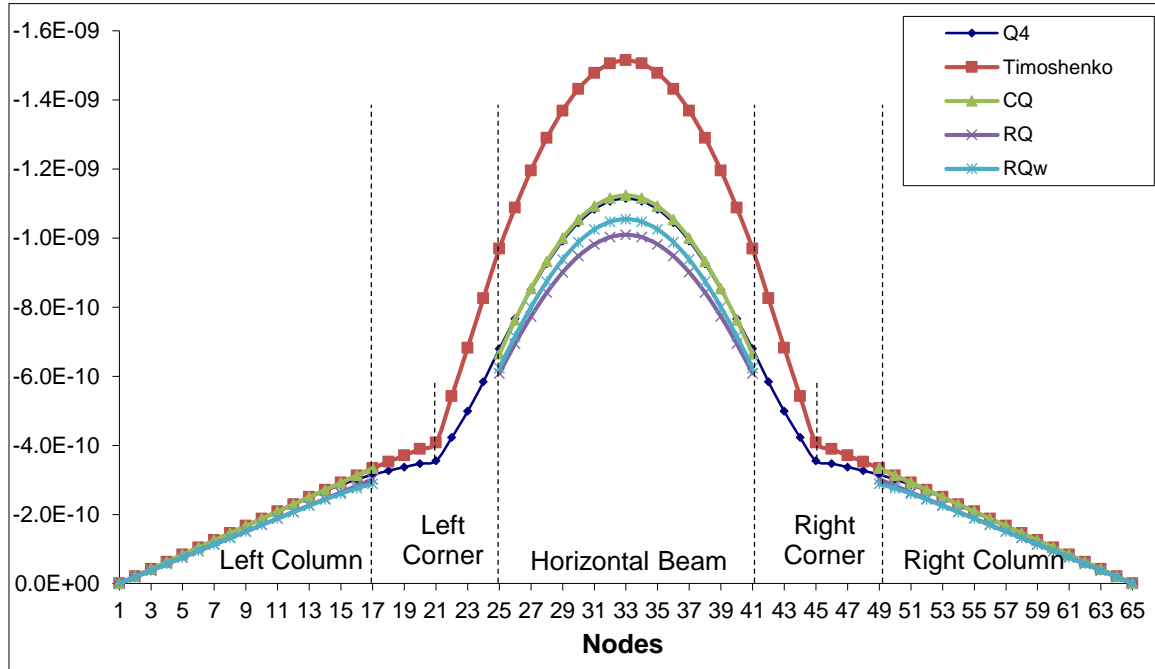


Figure 33: UY (m) displacement of the central line nodes along Y (load case 1)

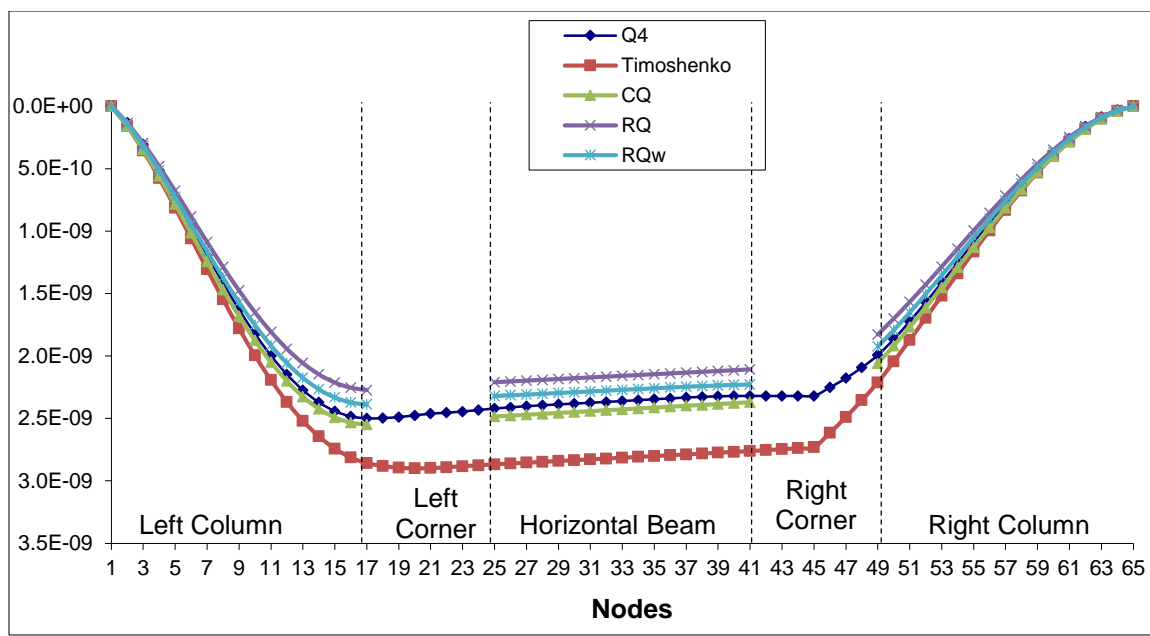


Figure 34: UX (m) displacement of the central line nodes along X (load case 2)

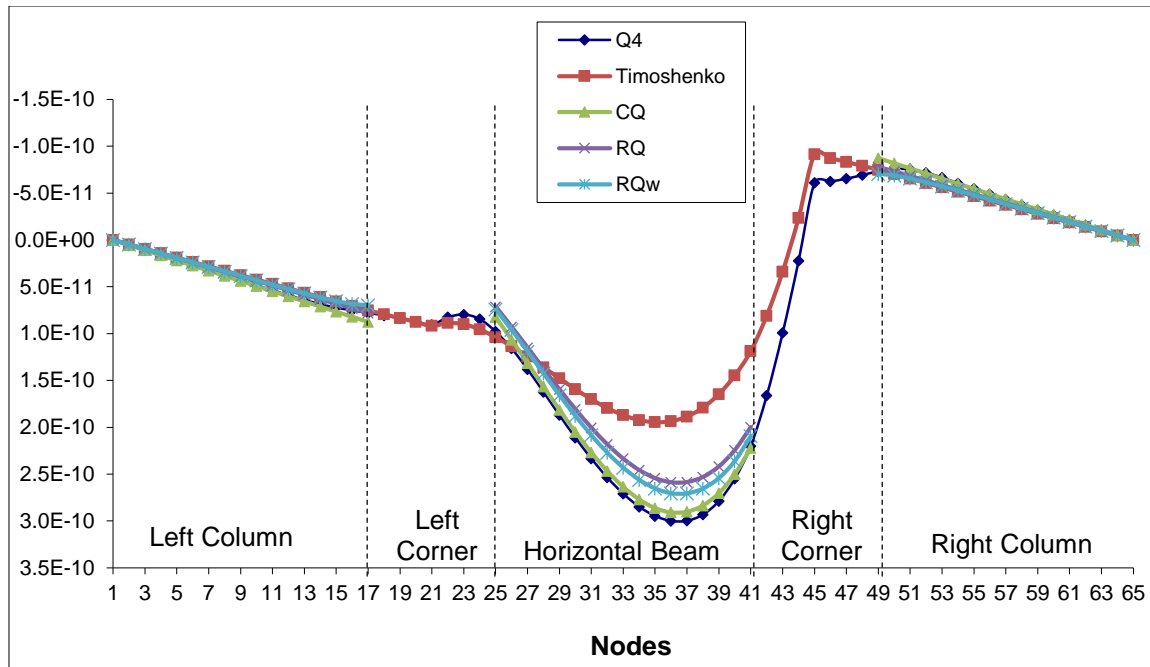


Figure 35: UY (m) displacement of the central line nodes along Y (load case 2)

The previous graphs show that the RQw is more flexible than RQ, whereas CQ gives best results.

3.6 Summary of the static analysis in the XY plane

The following table summarizes the results coming from all models (in the XY plan load):

Model	Node (où $E = E_{\max}$)	Load case	Displacement	E_{\max} par rapport à H8	E_{\max} par rapport à Q4
H8	15 ou 51	1	UX	0%	1.55%
H8	33	1	UY	0%	1.90%
H8	16	2	UX	0%	3.01%
H8	39	2	UY	0%	2.92%
Q4	15 ou 51	1	UX	1.55%	0%
Q4	33	1	UY	1.90%	0%
Q4	16	2	UX	3.01%	0%
Q4	39	2	UY	2.92%	0%
Timoshenko	14 ou 52	1	UX	15.22%	16.28%
Timoshenko	33	1	UY	38.45%	35.87%
Timoshenko	36 ou 37	2	UX	21.48%	18.19%
Timoshenko	38 ou 39	2	UY	28.44%	30.38%
CQ	15 ou 51	1	UX	1.52%	2.59%
CQ	17 ou 49	1	UY	2.74%	1.69%
CQ	28	2	UX	5.52%	2.70%
CQ	25	2	UY	4.48%	4.10%
RQ	14 ou 52	1	UX	6.30%	7.61%
RQ	33	1	UY	7.71%	9.44%
RQ	16	2	UX	6.48%	9.19%
RQ	37	2	UY	8.72%	10.97%
RQw	14 ou 52	1	UX	4.34%	5.71%
RQw	33	1	UY	4.34%	5.37%
RQw	17	2	UX	1.66%	4.52%
RQw	36	2	UY	6.77%	7.84%

Table 3: Comparison of all models and all load cases

It is obvious that the CQ model gives best results when comparing with the Q4 model.

3.7 Deformation in the plan perpendicular to the XY plane

In the case of a load along Z-axis, we will consider two new load cases:

- Load case 3: a uniform volumetric load of 78000 N/m³ along Z⁻ of the horizontal beam (shown in the next figure):

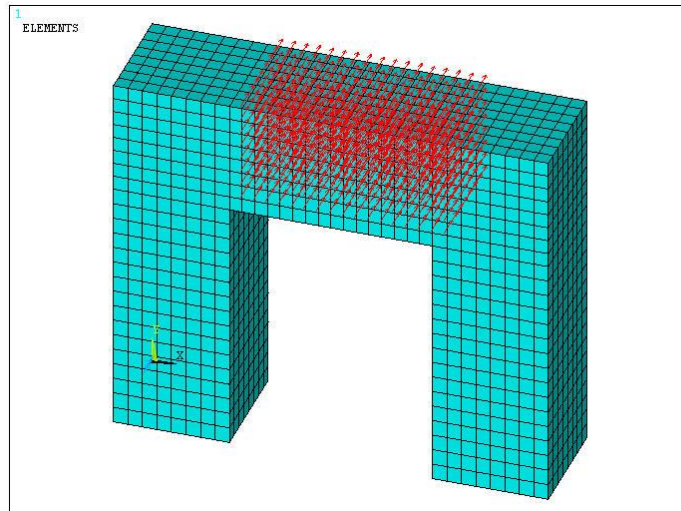


Figure 36: Test structure under load case 3 (3D view)

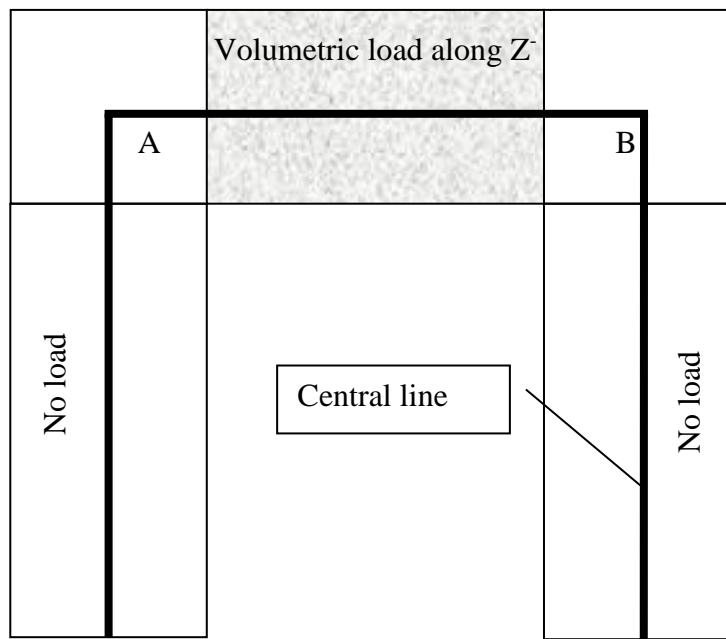


Figure 37: Test structure under load case 3 (2D view)

- Load case 4: a uniform volumetric load of 78000 N/m^3 along Z^- of the vertical left column (shown in the next figure):

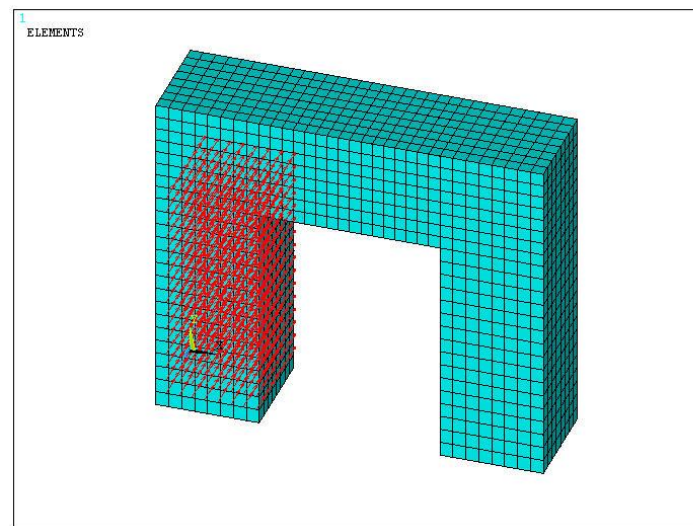


Figure 38: Test structure under load case 4 (3D view)

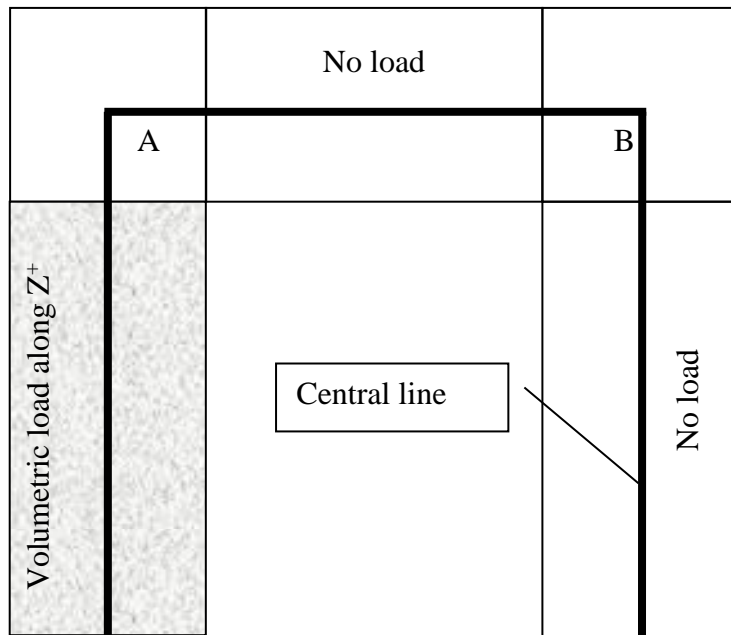


Figure 39: Test structure under load case 4 (2D view)

The following figures show the deformation under both load cases (3 and 4):

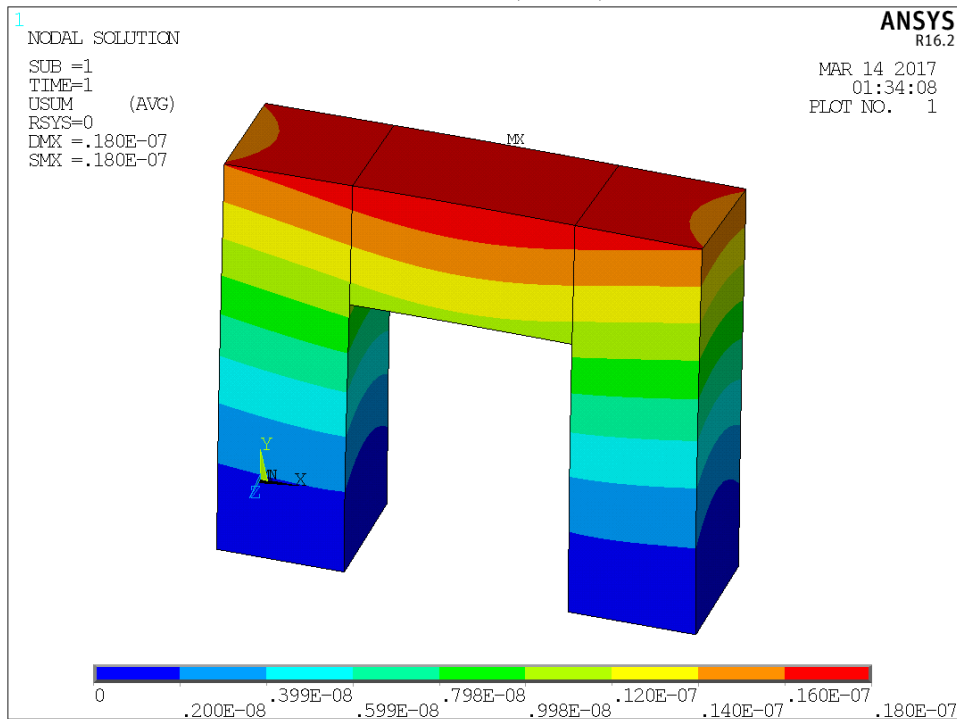


Figure 40 : Deformation of the volumetric model (under load case 3)

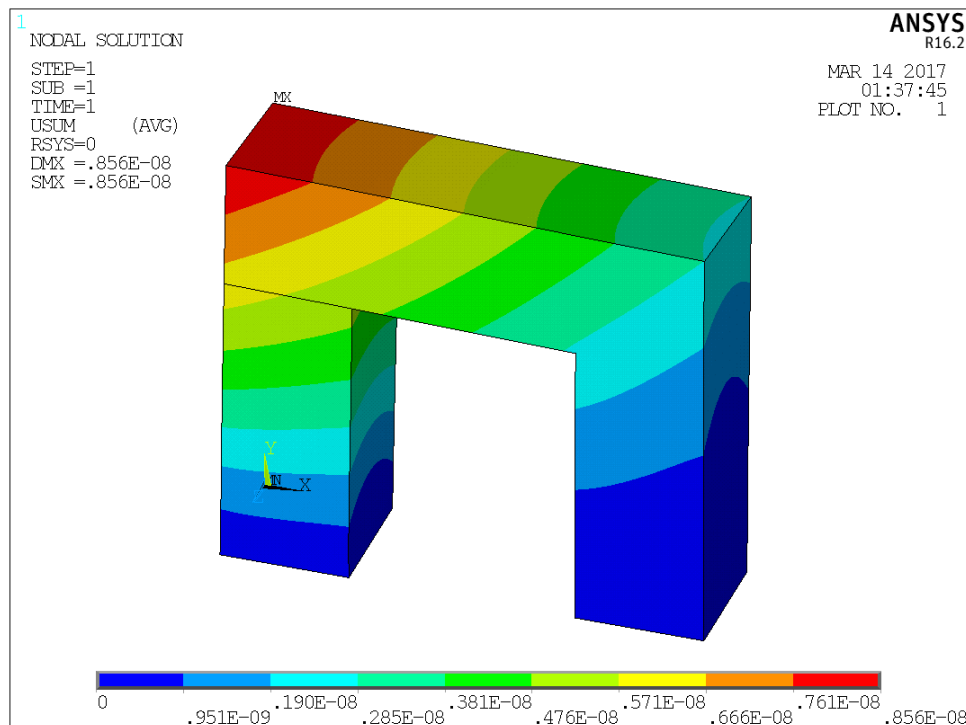


Figure 41 : Deformation of the volumetric model (under load case 4)

In these load cases, where the loads are along the Z axis, the Z displacements UZ will be used in the comparison. The reference model is the volumetric model using H8 finite elements. The linear 1D elements that we will test are:

- Timoshenko: this is the model that we have described earlier where we utilized 64 3D Timoshenko beam elements.
- Timoshenko+CPO: in this case, each corner is modeled with an oblique Timoshenko element (see next Figure). The columns and the horizontal beam are regular Timoshenko beam elements.

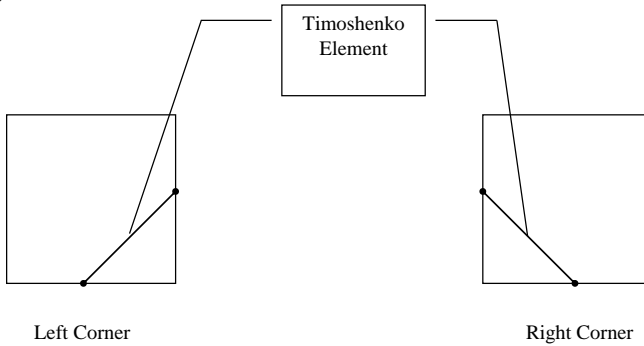


Figure 3-42 : CPO elements at the corners

- Timoshenko+CPO 1000E : where each corner is modeled by an oblique Timoshenko element with large rigidity (1000E), this will make the corner a rigid link.

The next figures show the results:

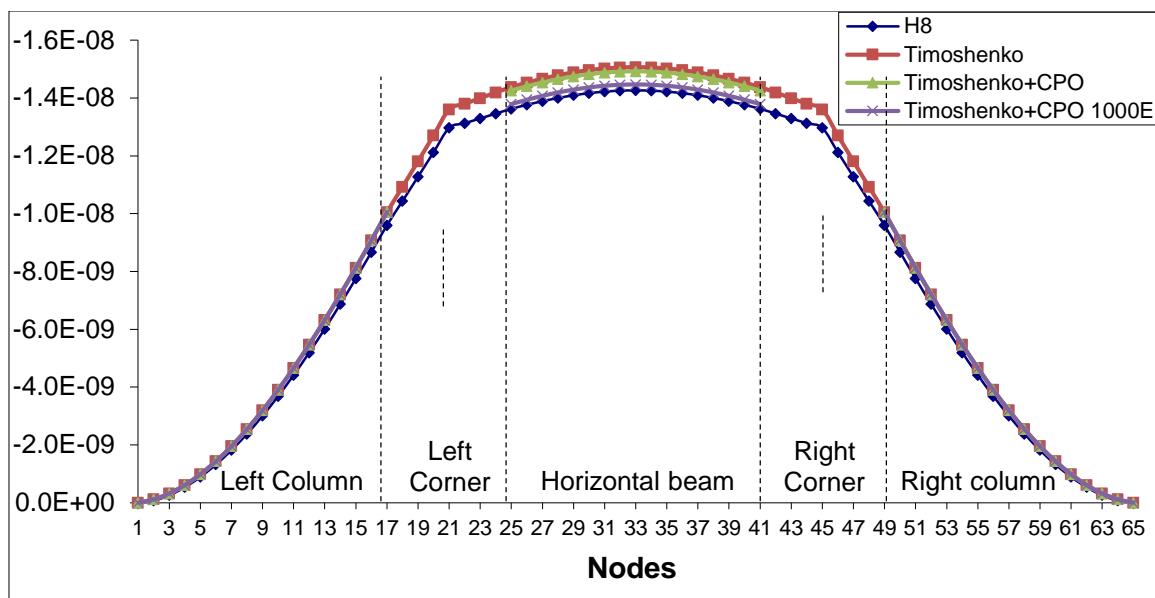


Figure 43 : Displacement UZ (m) of the nodes of the central line (load case 3)

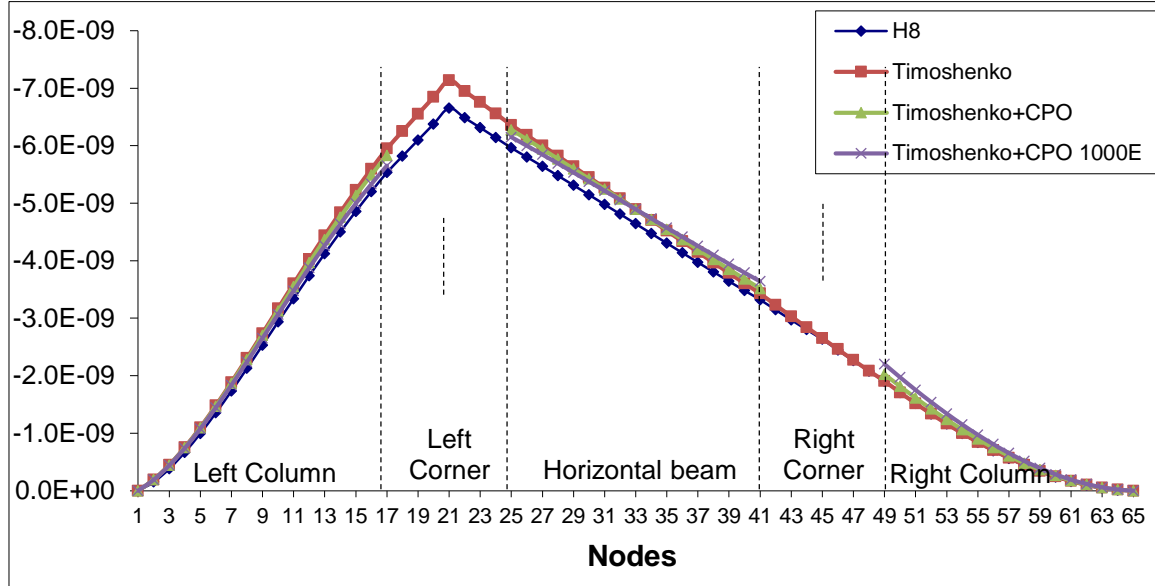


Figure 3-44 : Displacement UZ (m) of the nodes of the central line (load case 4)

The following table lists all results:

Model	Node (where $E = E_{\max}$)	Load case	Displacement	E_{\max} %H8
Timoshenko	33	3	UZ	5.59%
Timoshenko	17	4	UZ	6.26%
Timoshenko+CPO	33	3	UZ	4.59%
Timoshenko+CPO	25	4	UZ	4.70%
Timoshenko+CPO 1000E	17 ou 49	3	UZ	3.15%
Timoshenko+CPO 1000E	41	4	UZ	4.78%

Table 4: Comparison of displacements UZ of different models

It is clear that the results from the Timoshenko+CPO 1000E model are the closest when compared to the reference model the volumetric model (using H8 finite elements).

3.8 Conclusion of the static analysis

The load in the plan XY of the test structure modeled in linear finite element does not give any displacements of the nodes along the Z-axis nor rotations around the X-axis or the Y-axis. However, when the load is along the Z-axis of the structure will give displacements along the Z-axis and rotations around the X-axis and the Y-axis.

The results show that if we use CQ elements at the corners and Timoshenko beam elements everywhere else. However, when the load is along the Z-axis of the structure, rigid links at the corners and Timoshenko beam elements everywhere else will give best results in comparison to the volumetric modeling. This model performs very well in the static analysis; we still have to test it in the dynamic analysis.

4. DYNAMIC ANALYSIS

In this paragraph, the dynamical analysis of all models are again performed and the results are all compared. The modal analysis requires the calculation of the mass matrices of all models.

4.1 Error definition

During the modal analysis, we will calculate the relative error of the frequencies of vibration. It is defined as:

$$E_i = \frac{F_{Ri} - F_{Ci}}{F_{Ri}}$$

Where:

E_i = the relative error of the i^{th} mode of vibration

F_{Ri} = the frequency of the i^{th} mode of vibration of the reference model (Q4)

F_{Ci} = the frequency of the i^{th} mode of vibration of the new model

4.2 Mass matrix

a) Timoshenko beam

The elementary mass matrix of the Timoshenko beam with 2 nodes per element and 3 DOFs per node is given by:

```
m=rho*A*L/6*[  
2, 0, 0, 1, 0, 0  
0, 2, 0, 0, 1, 0  
0, 0, 0, 0, 0, 0  
1, 0, 0, 2, 0, 0  
0, 1, 0, 0, 2, 0  
0, 0, 0, 0, 0, 0];
```

(kwon, 2000)

b) Model Q4

The elementary mass matrix of the Q4 element with 4 nodes per element and 2 DOFs per node is given by:

```
m=rho*t*a*b/36*[  
4, 0, 2, 0, 1, 0, 2, 0  
0, 4, 0, 2, 0, 1, 0, 2  
2, 0, 4, 0, 2, 0, 1, 0  
0, 2, 0, 4, 0, 2, 0, 1  
1, 0, 2, 0, 4, 0, 2, 0  
0, 1, 0, 2, 0, 4, 0, 2  
2, 0, 1, 0, 2, 0, 4, 0  
0, 2, 0, 1, 0, 2, 0, 4];
```

(Cook, 2002)

c) Model CQ

The same method as for the static case is used to find the mass matrix of the corner element ($m = L^T \times M \times L$). The elementary mass matrix of the left corner element with 2 nodes per element and 3 DOFs per node is given numerically by:

```
mleft=[  
 1.0527e-002 -2.2619e-003 -1.0865e-005 7.0573e-003 1.5818e-003 2.8298e-006  
 -2.2619e-003 3.7758e-002 -8.2837e-005 2.9420e-003 7.0573e-003 -7.8169e-005  
 -1.0865e-005 -8.2837e-005 7.1917e-007 -7.8169e-005 2.8298e-006 3.1068e-007  
 7.0573e-003 2.9420e-003 -7.8169e-005 3.7758e-002 -2.2619e-003 -8.2837e-005  
 1.5818e-003 7.0573e-003 2.8298e-006 -2.2619e-003 1.0527e-002 -1.0865e-005  
 2.8298e-006 -7.8169e-005 3.1068e-007 -8.2837e-005 -1.0865e-005 7.1917e-007]
```

And with a simple transformation we can obtain the mass matrix of the right corner element of our test structure:

```
mrigh = [  
 1.0527e-002 2.2619e-003 -1.0865e-005 7.0573e-003 -1.5818e-003 2.8298e-006  
 2.2619e-003 3.7758e-002 8.2837e-005 -2.9420e-003 7.0573e-003 7.8169e-005  
 -1.0865e-005 8.2837e-005 7.1917e-007 -7.8169e-005 -2.8298e-006 3.1068e-007  
 7.0573e-003 -2.9420e-003 -7.8169e-005 3.7758e-002 2.2619e-003 -8.2837e-005  
 -1.5818e-003 7.0573e-003 -2.8298e-006 2.2619e-003 1.0527e-002 1.0865e-005  
 2.8298e-006 7.8169e-005 3.1068e-007 -8.2837e-005 1.0865e-005 7.1917e-007]
```

d) Model RQ

The mass matrix of a RQ element with 2 nodes per element and 3 DOFs per node is given by:

```
m=rho*t*a*b/9*4*[  
 6, 0, 0, 3, 0, 0  
 0, 6, 0, 0, 3, 0  
 0, 0, 32*b^2, 0, 0, 16*b^2  
 3, 0, 0, 6, 0, 0  
 0, 3, 0, 0, 6, 0  
 0, 0, 16*b^2, 0, 0, 32*b^2];
```

With :

a = length of the element = 0.045/16 = 0.0028125 m

b = height of the element = 0.02 m

t = thickness of the element = 0.02 m

rho = 7800 kg/m³

e) Model RQw

The mass matrix of a RQw element with 2 nodes per element and 5 DOFs per node is given by (warp in y and y²):

```
m=1/9*rho*t*a*b*2*[  
 12, 0, 0, -66*b^2, 0, 6, 0, 0, -33*b^2, 0  
 0, 12, 0, 0, 0, 6, 0, 0, 0, 0  
 0, 0, 64*b^2, 0, 646*b^4, 0, 0, 32*b^2, 0, 323*b^4  
 -66*b^2, 0, 0, 636*b^4, 0, -33*b^2, 0, 0, 318*b^4, 0  
 0, 0, 646*b^4, 0, 7636*b^6, 0, 0, 323*b^4, 0, 3818*b^6  
 6, 0, 0, -33*b^2, 0, 12, 0, 0, -66*b^2, 0  
 0, 6, 0, 0, 0, 12, 0, 0, 0, 0  
 0, 0, 32*b^2, 0, 323*b^4, 0, 0, 64*b^2, 0, 646*b^4  
 -33*b^2, 0, 0, 318*b^4, 0, -66*b^2, 0, 0, 636*b^4, 0  
 0, 0, 323*b^4, 0, 3818*b^6, 0, 0, 646*b^4, 0, 7636*b^6];
```

4.3 Summary of the dynamic analysis

The following table lists the relative errors of the frequencies (Hz) in comparison to the frequencies from the reference model (Q4):

Mode no	Shape	Q4	CQ	RQ	RQw	Timoshenko
1		4375.6	-0.1%	-5.6%	-3.0%	9.2%
2		12950	-0.8%	-5.8%	-4.3%	8.8%
3		17558	-2.2%	-6.3%	-5.6%	4.6%
4		18009	-0.4%	-5.8%	-3.9%	-2.4%
5		22432	-1.8%	-6.9%	-3.4%	8.2%
6		26894	-4.5%	-8.9%	-7.0%	3.0%
7		32996	-6.2%	-9.8%	-7.3%	-1.3%
8		40761	-4.4%	-9.1%	-5.4%	0.2%
9		48173	-7.5%	-12.7%	-9.0%	10.5%
10		51532	-3.8%	-5.1%	-2.6%	4.1%
Average			3.0%	7.1%	4.7%	5.4%

Table 5: The results (%Q4) of the dynamic analysis of the test structure.

To compare the results for all frequencies, we decided to find the average of the first 10 frequencies. It is clear that the CQ model gives the best results

5. CONCLUSION

Both analyses; the static and the dynamic analyses showed that when the loads are in the plan of the structure, best results are when we use CQ elements for the corners and Timoshenko beam elements for the other parts of the structure. However, the dynamical analysis stipulates to use Timoshenko beam elements when the vibrations are normal to the XY plane (the plane of the structure).

As we know 3D modeling gives more accurate results for both the static and the dynamic analyses. But this comes with a price. The price of large number of elements, large number of nodes, and eventually large number of DOFs. Replacing the volumetric modeling of a simple frame by traditional 1-D elements is the rule for performing static and dynamic analyses. In our frames, the connections are large enough that if we use regular linear beam elements, this is rise in a large difference between the 1D model and the reference model (volumetric H8 model). Using CQ elements at the corners improves the results of both the static analysis and the dynamic analysis. Consequently, the number of elements and the number of DOFs of the finite element model is radically reduced from hundreds of thousands to merely hundreds.

6. REFERENCES

- [1] Alghamdi, S. "Dynamic stiffness matrix and load functions of Timoshenko beam using the transport matrix", Computers and Structures, 79 (2001) 1175-1185.
- [2] Cook R. Concepts and applications of finite element analysis. 4th Edition. Wiley 2002.
- [3] Craig R. Structural Dynamics – An introduction to computer methods. John Wiley & Sons 1981.
- [4] Dohrmann CR, Key SW, Heinstein MW. A method for connecting dissimilar finite element meshes in two dimensions. International Journal For Numerical Methods In Engineering 2000; **48** (5), pp. 655-678.
- [5] Dohrmann CR, Key SW, Heinstein MW. Methods for connecting dissimilar three-dimensional finite element meshes. International Journal For Numerical Methods In Engineering 2000; **47**, pp. 1057-1080.
- [6] Hoit M. Computer Assisted Structural Analysis and Modeling. Prentice-Hall 1995.
- [7] Kassimali A. Structural Analysis. Second edition. Brooks/Cole 1999.
- [8] Kattner M, Crisinel M. Finite element modeling of semi-rigid composite joints. Computers and Structures 2000; **78**, pp. 341-353.
- [9] Quiroz L, Beckers P. Non-conforming mesh gluing in the finite elements method. International Journal For Numerical Methods In Engineering 1995; **38** (13), pp. 2165-2184.
- [10] Rao S. Mechanical Vibrations. 4th Edition. Pearson Education 2004.